

DRIVING STRESSES IN PRESTRESSED CONCRETE PILES

By Teddy J. Hirsch,¹ M. ASCE, Charles H. Samson, Jr.,² M. ASCE,
and Lee L. Lowery, Jr.,³ A.M. ASCE

ABSTRACT

Field tests were conducted to measure the dynamic stresses produced in prestressed concrete piles during driving. Strain gages were embedded in five 18-in. square piles 92 ft and 95 ft long, and two 15-in. square piles 26 ft long. The piles were tested at two sites on the Texas Gulf Coast, one near Corpus Christi and one near Houston, Texas. The field measurements are compared with the theoretical results obtained from a digital-computer solution of the wave equation. General conclusions as to the nature and magnitude of these stresses are drawn.

¹Assoc. Professor of Structural Engineering and Structural Mechanics, Dept. of Civil Engineering, and Assoc. Research Engineer, Texas Transportation Institute, Texas A&M University, College Station, Texas.

²Professor of Structural Engineering and Structural Mechanics, Depts. of Civil and Aerospace Engineering, and Head of Structural Research Dept., Texas Transportation Institute, Texas A&M University, College Station, Texas.

³Asst. Research Engineer, Structural Research Dept., Texas Transportation Institute, Texas A&M University, College Station, Texas.

TABLE OF CONTENTS

ABSTRACT	i
SYNOPSIS	1
INTRODUCTION	2
FIELD TESTS	4
Test Piles	4
Instrumentation	5
Soil Properties	6
Pile Driver	7
Cushioning Material	8
Pile Driving and Test Procedures	9
Test Data and Discussion	10
COMPUTER CORRELATION	15
General	15
Computer Results Compared with Field Data	15
PARAMETER STUDY	16
CONCLUSIONS	19
ACKNOWLEDGMENTS	21
REFERENCES	21

Specimens of concrete from the test piles were tested in order to determine their static and dynamic moduli of elasticity, compressive and tensile strengths, and unit weights. Specimens of the wood cushioning materials were also tested in order to determine their moduli of elasticity. Soil borings were made at the pile test sites in order to identify and determine the shear strength of the various soil strata. These material properties were used in setting up the pile problems for digital computer solution and in interpreting the significance of the measured dynamic stresses.

The effects of the soil conditions, pile properties, cushion material, and pile driving equipment on the driving stresses are discussed. Conclusions are drawn concerning driving conditions which are likely to produce large tensile and compressive stresses in prestressed concrete piles.

INTRODUCTION

During the year 1960-61, engineers of the Texas Highway Department Bridge Division engaged research engineers of the Texas Transportation Institute at Texas A&M University to develop a computer program to accomplish the mathematical calculations for the analysis of pile behavior during driving. With the aid of Edward A. Smith⁴ as a special consultant, a functioning computer program was developed and used successfully on a number of pile problems.^{5,6,7} This program was prepared for the IBM 709 Computer at the Texas A&M University Data Processing Center. With the use of this program, it is practical to investigate theoretically the behavior of various type piles when driven by different equipment under different foundation conditions.

⁴Formerly Chief Mechanical Engineer for Raymond International Inc., now retired.

⁵"Pile-Driving Analysis by the Wave Equation (Computer Procedure)," by Charles H. Samson, Jr., Report RP 25, Texas Transportation Institute, Texas A&M University, May, 1962.

⁶"Computer Study of Dynamic Behavior of Piling," by Charles H. Samson, Jr., Teddy J. Hirsch, and Lee L. Lowery, Jr., a paper presented to the Third Conference of Electronic Computation, ASCE, Boulder, Colorado, June, 1963.

⁷"Stresses in Long Prestressed Concrete Piles During Driving," by Teddy J. Hirsch, Report of the Texas Transportation Institute, Texas A&M University, September, 1962.

In order to properly use this theoretical solution of the wave equation, it was considered necessary to conduct field tests to obtain actual stress and displacement data to correlate with the theory. During the 1961-62 year, three prestressed concrete piles 95 ft in length and two piles 92 ft in length were instrumented with strain gages and displacement transducers and tested during driving. The field tests were conducted on the Nueces Bay Causeway at Corpus Christi, Texas.

During the 1962-63 year, two prestressed concrete piles 26 ft in length were tested to obtain data on the stresses and displacements of relatively short piles. These tests were conducted at the construction site of the McHard Underpass on Interstate Highway 45 South of Houston, Texas.

Published data of stresses in piles during driving are very limited because of the expense and difficulties involved in installing strain gages on piles and testing them. Glanville, Grime, Fox, and Davies⁸ measured stresses in reinforced concrete piles from 15 to 50 ft long in 1938. The American Railway Association⁹ measured the dynamic stresses in hollow steel piles 65 to 110 ft long in 1949.

The purpose of this paper is to present the strain gage techniques used and results obtained in field tests on prestressed concrete piles, and to briefly discuss the application of wave theory to the structural analysis and design of prestressed concrete piles. The magnitude of the dynamic tensile stresses in prestressed concrete piles is extremely important since these piles are vulnerable to cracking during driving. Such piles are frequently designed on the basis of handling stresses only, but

⁸"An Investigation of the Stresses in Reinforced Concrete Piles During Driving," by Glanville, W. H., Grimes, G., Fox, E. N., and Davies, W. W., British Building Research Board Technical Paper No. 20, Dept. of Scientific and Industrial Research, His Majesty's Stationery Office, London, 1938.

⁹"Steel and Timber Pile Tests-West Atchafalaya Floodway-New Orleans, Texas and Mexico Railway," American Railway Engineering Association, Bulletin 489, September-October, 1950.

the occurrence of breakage during driving has caused designers to increase the amount of prestress. The magnitude of the prestress force that should be used under various driving conditions is very controversial.

FIELD TESTS

Test Piles. Strain gages were embedded in seven prestressed concrete piles and the dynamic stresses produced during driving were recorded on a multi-channel recording oscillograph. The dimensions and design properties of the two test piles are presented in Figures 1 and 2.

Test Piles 1, 2, 3, and 4 were 18 in. square with a 9-in. hole running longitudinally. Each of these piles had three strain gages cast in them as shown in Figure 2. These gages were not at the center of gravity of the cross section and consequently would pick up flexural stresses in addition to axial stresses.

Test Pile 5 was also 18 in. square with a 9-in. hole running longitudinally; however, this pile had two strain gages placed on opposite sides of the cross section so that the axial and flexural stresses could be determined from the stress records. Gages were installed in this manner near the head of the pile and near the one-third point. Test Piles 1, 2, and 3 were 95 ft long and Test Piles 4 and 5 were 92 ft long.

Test Piles 6 and 7 were 16 in. square and 26 ft long. These two piles had gages located at five points along their length. Two gages at each location were hooked up as opposing arms of the wheatstone bridge used to measure strain. In this manner bending stresses were eliminated and only axial stresses on the pile cross section were recorded at each gage point.

Concrete specimens were obtained as the piles were being cast. Values of the unit weight, compressive strength, tensile strength, modulus of rupture, modulus of elasticity, and Poisson's ratio are presented in Table 1.

TABLE 1. Properties of Concrete in Test Piles

Property	Test Pile		
	1, 2 & 3	4 & 5	6 & 7
Unit Weight, pcf	158	154	154
Compressive Strength, psi	8490	8060	6570
Tensile Strength, psi (Direct Tension Test)	455	465	520
Modulus of Rupture, psi (Center-point Test)	925	790	1120
Modulus of Elasticity, psi			
Static Test	8.18×10^6	6.95×10^6	7.67×10^6
Dynamic Test	8.32×10^6	7.71×10^6	7.84×10^6
Poisson's Ratio (Dynamic)	.15	.16	.21

Note: Values for Test Piles 1, 2, 3, 4, and 5 were 42-day tests.
 Values for Test Piles 6 and 7 were 28-day tests.

The modulus of elasticity of the concrete was required to transform the strain gage readings into stress. Both the modulus of elasticity and unit weight values were used in setting up these pile problems for the theoretical solutions by use of the digital computer. The strength properties are useful in interpreting the significance of the measured dynamic stresses.

Test Piles 1, 2, 3, 4, and 5 were cast by Ross Anglin and Son, General Contractors at Corpus Christi, Texas. Test Piles 6 and 7 were cast by Baass Brothers Concrete Company at Victoria, Texas

Instrumentation. Baldwin AS-9 constantan wire gird, Valore type brass foil envelope, strain gages were embedded parallel to the longitudinal axis of the precast prestressed concrete piles during the placing of the concrete. This was done about four weeks prior to the driving of

the piles. Two different types of lead wire were used for the tests. The one which proved most satisfactory was Belden No. 8404, AWG No. 20, four conductor, shielded, vinyl plastic covered cable. These lead wires were run the length of the piles embedded in the concrete and were brought out near the pile head. Since the length of the lead wires, gage locations, and manner of hookup had been determined prior to the installation of the gages, strain gage connections and connectors were prepared and waterproofed in the laboratory. The lead wire and strain gage connections were soldered and then embedded in Armstrong A-2 epoxy adhesive for insulation and waterproofing. These connections were then covered with microcrystalline wax for additional moisture proofing. Connectors were soldered to the other end of the lead wires and these were sealed in plastic bags to protect them from the weather prior to testing.

No gluing, soldering, or waterproofing was done in the field. This was necessary since all instrumenting and testing had to be performed under field construction conditions such that the contractor would not be unduly delayed. About 15 minutes was required for two men to install the strain gage assemblies on each of the piles.

A Consolidated Electrodynamic Corporation Type 5-116 Recording Oscillograph and two CEC Type 1-118 Carrier Amplifier systems were used to record the dynamic strains in Test Piles 1, 2, 3, 4, and 5. The oscillograph was equipped with CEC Type 7-323 Galvanometers having a flat frequency response to 600 cycles per sec. A Honeywell Type 1508 Visicorder oscillograph and a Honeywell Type 119 Carrier Amplifier system were used to amplify and record the dynamic strains and displacements of Test Piles 6 and 7. This oscillograph was equipped with Honeywell Type M1650 Galvanometers having a flat frequency response to 1000 cycles per sec. The required 110 volts, 60 cycle, electrical power was supplied by a portable generator.

A Bourns Model 108 linear motion potentiometer with a 6 in. travel was used to record the dynamic displacements in Test Piles 6 and 7. These data were recorded on the oscillograph with the strain gage data.

Soil Properties. The identification, description, and shear strength properties of the soil into which the piles were driven are presented in Figure 3.

Test Piles 1, 2, 3, 4, and 5 (95 ft long and 92 ft long) were driven into soft marine deposits on Nueces Bay at the mouth of the Nueces River near Corpus Christi, Texas. The soil down to about 65 ft depth was soft clay, loose silty, sandy material. Below about 65 ft a firm sandy and gravelly

material was encountered. The foundation exploration crews of the Texas Highway Department drilled the soil test holes. In general, the Texas Highway Department "in place" vane shear and the THD standard penetrometer test were found to be most practical for the Nueces Bay area. Very frequently the undisturbed sample required for a triaxial or "miniature vane" test could not be recovered from the sampling tube. These various methods of tests appeared to yield values in reasonable agreement with each other. The average unit weight of this material was about 115 pcf and the submerged effective weight was about 52.6 pcf. A summary of the test results is presented in Figure 3.

Test Piles 6 and 7 (26 ft in length) were driven in a firm clay deposit, south of Houston, Texas. The ultimate shear strength and description of the soil at various depths in the ground are also given in Figure 3.

Pile Driver. The manner in which a pile driver delivers its driving energy to a pile has a significant effect on the stresses produced. The driving energy of simple drop hammers and single acting steam hammers results from the impact of the ram on the pile. In the field tests, a Delmag diesel pile driver Type D-22 was used. This hammer has a manufacturer's rated energy output per blow of 39,700 ft-lb. The technical data concerning this hammer are given in Table 2.

TABLE 2. Technical Data for Delmag D-22 Diesel Hammer¹⁰

Piston weight	4,850 lb
Weight of hammer	9,768 lb
Weight of anvil	1,147 lb
Number of blows per minute	42-60
Energy output per blow	39,700 ft-lb
Maximum explosion pressure on pile	158,700 lb

The working principles of the diesel pile hammer are shown in Figure 4. The driving force delivered to the pile results from two events: the impact of the ram on the anvil, and the explosion of the diesel fuel. By far the greater of these two forces is the impact of the falling ram on the anvil. This force depends on the weight of the ram and its velocity at impact. In order to

¹⁰"Delmag Diesel Pile Hammers-Technical Data," Goddard Machinery Company Inc., Houston, Texas.

determine this velocity, it is necessary to know the height of fall of the ram. Referring to Figure 4, one sees that the ram is free falling until it passes the exhaust ports on the side of the diesel cylinder. After mathematically investigating the effect of the compressed diesel fuel on the ram velocity, the investigators concluded that the velocity of the ram at impact is essentially the same as the free-fall velocity at the instant it passes the exhaust ports. Therefore the ram velocity at impact can be approximated by

$$V = \sqrt{2g(h - 1.25)}$$

in which

V = ram velocity in ft/sec,

g = acceleration due to gravity (32.2 ft/sec²),

h = total fall of ram in ft, and

1.25 = distance from center of exhaust port to anvil striker face in ft.

This equation is used to determine the ram velocity for the theoretical solution of driving stresses. In addition to the energy transmitted to the pile by the falling ram, the energy created by the explosion pressure of the diesel fuel is included in the theoretical computations. This is approximated by holding the maximum explosion pressure of 158,700 lb on top of the anvil for a period of 0.01 sec after the initial ram impact. The duration of the explosion was investigated by M. Rands.¹¹

Cushioning Material. In the driving of concrete piles, the cushion block between the helmet and the top of the pile is of major importance. The magnitude of the driving stresses are directly dependent upon the stiffness of this material.

Test Piles 1, 2, 3, 4, and 5 were driven using a green oak cushion 18 in. square and 6.5 in. thick. The driving force was applied perpendicular to the grain. After several hundred hammer blows, it was compressed to a thickness of about 4.5 in. Laboratory tests indicated its static secant modulus of elasticity in this state to be about 40,000 psi. A typical stress-strain curve is given in Figure 5. The coefficient of restitution of the material was 0.8 under a static load test. Other investigators have reported a dynamic coefficient of restitution for oak ranging from 0.25 to 0.5.

Test Piles 6 and 7 were driven using a pine plywood cushion 16-in. square and 4 in. thick. The driving force was applied perpendicular to its grain and after several hundred blows, it was compressed to

about 3 in. Laboratory tests on this type material indicated that its static secant modulus of elasticity was also about 40,000 psi.

Pile Driving and Test Procedure. When the test piles arrived at the driving site by truck, the strain gages had been previously cast in them and several feet of lead wires with connectors attached were protruding from the concrete near the pile head. Shielded cable extensions were connected to these wires, and the pile was then raised into position in the leads of the pile driver rig. The extension cables were connected to the amplifiers of the recording oscillograph, and each strain gage channel was balanced and calibrated prior to the driving of the pile.

The piles had been previously measured and marked at one-foot intervals so that the penetration of the pile into the ground could be determined. As the pile was being driven continuously into the ground, the recording oscillograph was turned on intermittently at different depths of penetration. In general, the recorder was run for periods of 3 to 5 sec. By doing this the stresses from three to five consecutive blows could be recorded along with the time interval between blows. This time interval was desired since it permitted the height of the ram fall to be more accurately determined than from direct visual observations.

On Test Piles 1, 2, 3, 4, and 5 the average penetration per blow was determined from level readings on the pile during driving. On Test Piles 6 and 7 a linear motion potentiometer was used to determine the penetration per blow.

After the pile had sufficiently penetrated the ground and the permanent set was about 1 in. per blow, the pile driver was stopped and the displacement transducer was attached. One end of the transducer was attached to the pile with a clamp and its base was attached to a timber resting on piles previously driven. The pile driver was then started and run for about six to seven blows and the dynamic stresses and displacements were recorded.

The entire field procedure was designed such that the data could be obtained in a manner that would not unduly delay the contractor. This was necessary since the contractor received no monetary compensation for his cooperation in this pile research.

Figures 6 and 7 show the diesel hammer driving a 95 ft prestressed concrete pile. Figure 8 shows the CEC recording oscillograph and strain gage amplifier unit.

Test Data. Figure 9 gives an example of the oscillograph record of the dynamic strains in Test Pile 3. This pile had penetrated 45 ft into the ground. Gage 1 was located near the head of the pile, gage 2 at mid-point of the pile, and gage 3 near the point of the pile. The maximum recorded compressive stress occurred at gage 1 and was about 2,270 psi. The maximum measured tensile stress was about 860 psi and occurred at gage 2. The vertical lines on Figure 9 are time lines and are spaced at 0.01 sec intervals. The time required for the stress wave to travel from gage 1 to gage 3 (76 ft) is about 0.0058 sec. The velocity of this stress wave was about 16,300 ft per sec and the longitudinal frequency of vibration is about 86 cycles per second. This compressive wave is seen to be reflected from the pile point as a tensile wave. This can cause tensile breakage in prestressed concrete piles being driven in soils offering little point resistance.

Figure 10 is also an oscillograph strain record from Test Pile 3. However, in this case the pile had penetrated 74 ft into the ground. In comparing this record with that of Figure 9, it is interesting to note how little tensile stress occurred at gage 2 when the pile was 74 ft in the ground. It is apparent that the increased point resistance shown by gage 3 (also see Figure 3) decreased the magnitude of the reflected tensile wave. It is probable that the damping effect of the increased soil resistance also contributed to decreasing the reflected tensile stress wave.

If a pile encounters little or no soil resistance, a theoretical analysis would indicate the reflected tensile stress wave would have a magnitude equal to the initial compressive stress wave. This of course would cause tensile breakage of most prestressed concrete piles. This leads to a conclusion that prestressed concrete piles are most vulnerable to breakage at the beginning of driving when little soils friction and point bearing are encountered.

Test Piles 1, 2, 3, 4, and 5 had a final prestress of about 800 psi, and the concrete had an additional tensile strength of about 460 psi. This indicates these piles should withstand a measured tensile stress of about 1260 psi without failure. Keeping this in mind, it is interesting to look at Table 3, which summarizes the maximum tensile and compressive stresses recorded in the test piles. The maximum tension recorded in the 95-ft and 92-ft piles was 1350 psi in Test Pile 2; however, values of around 900 to 1100 psi were common. The net tensile stress in the concrete can be determined by subtracting the prestress from the measured values.

These measurements are interesting in view of the fact that two piles broke in tension while being driven within 200 ft of Test Piles 1, 2, and 3. Figures 13 and 14 show these broken piles. All the tensile cracks were located in the lower half of the piles. Some cracks were also at the mid-point of these piles. These observations will be further discussed later.

Figure 11 is an oscillograph strain record of Test Pile 5 that shows the presence of bending in the pile. Gages 1 and 2 were located at the head of the pile but on opposite sides of the cross section. Gages 3 and 4 were located about 32.5 ft from the pile head on opposite sides of the cross section also. The maximum compression at gage 1 was 2,020 psi, while gage 2 shows 1,665 psi. This indicated bending stresses at the pile head of about ± 177 psi. The maximum compression at gage 3 was 1,925 psi, while gage 4 shows 1,225 psi. At this point on the pile the bending stresses associated with the compressive wave are about ± 350 psi. The maximum tension at gage 3 was 700 psi, while gage 4 shows 415 psi. At this point on the pile the bending stresses associated with the tensile wave are about ± 142 psi. Such bending stresses may be attributed to several factors: hammer not centered on top of pile, crooked pile, pile not vertical, and top of pile out of square.

Test Piles 6 and 7 (26 ft long) were instrumented in a manner such that only axial stresses were recorded at each gage point. Two strain gages were positioned at each point on opposite sides of the cross section. These two strain gages were hooked up on opposing arms of a wheatstone bridge and in this manner bending stresses were automatically averaged out. Figure 12 gives an example of the oscillogram of the dynamic strains and displacements for Test Pile 7. This pile had penetrated 19 ft into the ground. Gage 1 was located at the head of the pile, gage 2 at the quarter point, gage 3 at the mid-point, gage 4 at the three-quarter point, and gage 5 at the point of the pile. The displacement transducer was attached about 5 ft below the pile head.

The maximum compressive stress occurred at gage 1 and is about 2,576 psi. The maximum tensile stress occurred at gage 3 and is about 464 psi. The maximum displacement is about 0.7 in., and the permanent set about 0.6 in. Thus the temporary elastic compression of the ground and pile is about 0.1 in. in this case. The vertical lines on the figure are time lines and are spaced at 0.01 sec intervals. The longitudinal frequency of vibration is seen to be about 283 cycles per sec. This results in a stress wave velocity of about 14,750 ft per sec.

The two 26 ft piles had a final prestress of about 710 psi and the concrete had a tensile strength of about 520 psi. This indicates these piles should withstand a measured tensile stress of about 1,230 psi without failure. The compressive strength of the concrete was about 6,570 psi. Keeping this in mind, it is interesting to note Table 3, which gives a summary of the maximum tensile and compressive stresses

TABLE 3

Maximum Measured Compression and Tensile Stresses
Prestressed Concrete Piles

Depth of Pile in Ground ft	Computed Hammer Drop ft	Average Penetration per Blow in	Maximum Stresses*	
			Compression psi	Tension psi
Test Pile 1 (95 ft long)				
48-	4.55		2045	982
48	3.95		1922	982
48-51	4.15		1840	1145
51	4.45		2086	1063
55	4.48	1.57	2086	982
55+	5.14	1.57	2086	1022
59	4.74	1.03	1963	1022
63	4.61	1.188	1963	1022
64+	4.87	1.18	1677	1022
68	4.66	.781	1759	614
68.5	4.96	.638	1759	245
69	5.18	.495	1800	123 (gage 1)
69.7	5.38	.298	1840	123 (gage 1)
71	4.78	.075	1513	0
73.5-	4.96	.064	2127	409
73.5	5.05	.064	2209	450
74.8	5.14	.079	2413	654
Test Pile 2 (95 ft long)				
34	4.35		1840	1350
42	3.82		1513	1186
49	3.48	2.77	1268	900
55	3.37	1.77	1227 (gage 2)	818
58	3.68	1.41	1267 (gage 2)	900
63-	3.63	1.34	1391	859
63	3.81	1.34	1432 (gage 2)	982
67	3.94	1.28	1513	941
68	4.40	1.04	1718 (gage 2)	982
Test Pile 3 (95 ft long)				
7	5.40		2147	828
8	5.12		2209	736
10	4.92		2270	767
12	4.74		2393	798
17	4.25	1.338	2239	982

*Maximum compressive stress occurred at head of pile unless noted otherwise.
Maximum tensile stress occurred at mid-point of pile unless noted otherwise.

TABLE 3 (Continued)

Depth of Pile in Ground ft	Computed Hammer Drop ft	Average Penetration Per Blow in	Maximum Stresses	
			Compression psi	Tension psi
35	3.94	4.99	1932	920
40	3.48	2.90	1564	675
45	4.19	2.81	2178	890
50	3.78	2.34	2239	828
55	4.19	1.91	2117	859
60	4.09	1.60	2147	859
65	4.18	1.61	2178	920
67	4.02	.89	2147	828
68	4.14	.46	2209	736
68+	4.42	.46	2179	644
69	4.36	.233	2270	614
70-	5.12	.135	2883	644
70	5.42	.135	3006	644
70+	4.48	.135	2362	460
74	4.48	.055	2239	338
74+	4.39	.055	2178	276

Test Pile 4 (92 ft long)

20	4.18	.923	1642	599
23	3.78	12.0	1798	964
46	4.18	2.40	2007	834
50	4.26	.308	2007	782
52	4.26	.154	2033	599
53	4.43	.138	2059	495
54	4.43	.10	2007	521
55	4.02	.247	1772	704
56	4.18	.308	1824	782
57	4.18	.353	1824	964
65	3.63	.571	1147	521
66	4.78	.364	2007	443
69	4.78	.104	1981	443

Test Pile 5 (92 ft long)

5	3.94		1876	1053
10	3.78	1.00	1826	1091
15	3.70	3.00	1849	1294
20	4.02	.705	1852	1053
25-35	3.94	7.50	2016	1192
40	3.94	2.00	1806	891
45	3.86	2.40	1832	911

TABLE 3 (Continued)

Depth of Pile in Ground ft	Computed Hammer Drop ft	Average Penetration per blow in	Maximum Stresses	
			Compression psi	Tension psi
50	4.52	.364	2060	775
54	4.26	.174	2168	728
55	4.26	.292	2071	722
57	4.18	.48	1988	921
58	4.10	.667	1982	1005
61		.75	1797	735
65	4.26	.75	2102	1087
67	4.60	.4	2354	965
68	4.69	.15	2380	824
69	4.69	.074	2342	668
69.5	4.52	.06	2206	494
70	4.60	.052	2136	436
Test Pile 6 (26 ft long)				
2	3.80		1514 (gage 2)	358 (gage 4)
3	5.13		2452	472 (gage 4)
12	4.87		2208	488 (gage 4)
15	5.22		2543	358 (gage 4)
19	5.68		2772	407 (gage 4)
20	5.70		2818	358 (gage 4)
22.5	6.34	0.69	3350	495
24	6.06		2970	456
Test Pile 7 (26 ft long)				
2	3.45		1818	618
11	4.79		2121	464
15	5.27		2379	464
18	6.56	0.66	2906 (gage 2)	541
19	5.60	0.53	2906 (gage 2)	696
20	5.68		2738 (gage 2)	387
25	5.27		2788	541

recorded in these two piles. The maximum tensile stress recorded was 696 psi in Test Pile 7; however, values of around 400 to 600 psi were more common. The maximum compressive stress recorded was 3,350 psi in Test Pile 6; however, values of around 2,500 to 2,900 psi were more common.

The net tensile stress in the concrete can be determined by subtracting the prestress from the measured stress. If this is done, it becomes apparent that these short piles experienced no net tensile stress.

In general, the magnitude of the tensile stresses in the 26 ft piles was only about one-half of those measured in the 92 ft and 95 ft piles. The compressive stresses in the short piles were slightly greater than those in the long piles, but this was probably because of the different cushions used.

COMPUTER CORRELATION

General. In order to correlate the field data with theoretical results, these pile problems were run on an IBM 709 Digital Computer. For the computer solution, a pile is simulated as shown in Figure 15. Test Piles 6 and 7 were divided into eight elements as shown in Figure 15. However, Test Piles 1, 2, 3, 4, and 5 were divided into 20 discrete elements because of their greater length. The program used was essentially the same as that described by E.A.L. Smith¹² and in previous work by the writers,⁶ except that it has been modified to include the effect of gravity and separate frictional point forces on the last pile segment. To accomplish the problem simulation, various physical data concerning the ram, anvil, capblock, helmet, cushion, pile, and soil were necessary. Much of the data was obtained from the pile driver manufacturer, field observations, and laboratory tests and is reported in this paper. However, data concerning the dynamic stress-strain characteristics of the wood, concrete, and soil are practically nonexistent, and engineering estimates were necessary.

E. A. L. Smith¹² suggested that the use of internal damping in the pile material might be desirable to account for energy losses due to a stress-strain hysteresis. Although no data were available that suggested a value for such a damping property of concrete, values were assumed in these problems.^{6,7,11} Soil quake and damping constants that simulate dynamic stress-strain behavior were also assumed.^{6,7,11,12} Future research work is planned which should more clearly define and evaluate these now elusive parameters.

Computer Results Compared with Field Data. A comparison of the computed stresses and displacements with those measured in the field is

¹²Smith, E.A.L., "Pile-driving Analysis by the Wave Equation," Journal of the Soil Mechanics and Foundations Division, Proceedings of the American Society of Civil Engineers, Volume 86, Number SM 4, pp. 35-61, August, 1960.

given by Table 4. Since the strain gages were located at various points along the length of the pile, the computed stresses shown were taken from the corresponding segments of the pile. The compressive stresses tabulated were taken from the gage nearest the head of the pile and the tensile stresses tabulated were taken from the gage nearest the mid-point of the pile unless noted otherwise. For the exact location of these gages, reference is made to Figures 1 and 2. The comparison was made in this manner, because in general the maximum measured compressive stress was near the pile head and the maximum measured tensile stress was near the mid-point of the pile. This is not to be construed to mean that these were the maximum stresses present in the pile. The theoretical analysis often indicated larger tensile stresses at points other than where strain gages were located. The computer analysis indicated the 95 ft and 92 ft piles had larger tensile stresses in their lower half. The two fractured piles, shown by Figures 13 and 14, tend to support this observation. The measured stresses shown are the average of several consecutive blows.

To make a qualitative comparison of the computer results with the recorded oscillograph stress data, Figures 16, 17, 18, and 19 are presented. These figures show a computer plot of the stress versus time for segments at the head and mid-point of Test Piles 3 and 7. They are the same oscillographs shown in Figures 9 and 12 respectively, except the scales have been changed.

Figure 20 shows a comparison of the computed displacement of the pile head with the measured displacement (oscillogram shown in Figure 12).

While it may be argued that these comparisons leave something to be desired, they are very reasonable considering the large number of variables affecting the dynamic behavior of piles. There are some 21 variables which have been considered in the theoretical analysis by the wave equation. Because of the nature of the field tests, close control of the values of the variables was not possible. For example, it is known that the diesel hammer does not deliver its energy in exactly the same manner on successive blows, the properties of the wood capblock and cushion are constantly changing during driving, and the dynamic stress-strain properties of the wood, concrete, and soil materials were estimated from rather limited test data. Even so, these comparisons indicate the use of the numerical solution of the wave equation developed by E.A.L. Smith is a rational and sound procedure for determining the dynamic behavior of piles during driving.

PARAMETER STUDY

The computer program has been used to determine the effects of ram weight, ram energy output, cushion stiffness, pile cross-sectional area,

TABLE 4

Comparison of Computed Stresses with Measured Stresses

Depth of Pile in Ground ft	Computed Hammer Drop ft	Average Penetration Per Blow in		Comparison of Computed Stresses with Average Measured Stresses			
		Comp.	Meas.	- Compression* psi		+ Tension* psi	
				Comp.	Meas.	Comp.	Meas.
Test Pile 1 (95 ft long)							
48	4.55	.259		-2393	-1992	+ 673	+ 929
51	4.45	.227		-2365	-1944	+ 645	+ 896
55	4.19	.180	1.57	-2283	-2031	+ 549	+ 995
59	4.74	.177	1.03	-2462	-1909	+ 693	+ 954
68	4.66	.137	.781	-2353	-1677	+ 513	+ 592
71	4.78	.130	.075	-2465	-1486	+ 588pt	+ 573pt
74	5.14	.104	.079	-2367	-2372	+ 321	+ 627
Test Pile 2 (95 ft long)							
34	4.35	.333		-2338	-1620	+ 762	+1096
42	3.82	.274		-2159	-1317	+ 555	+ 924
49	3.48	.198	2.77	-2037	-1353	+ 436	+ 810
58	3.68	.147	1.41	-2118	-1200	+ 428	+ 886
63	3.81	.138	1.34	-2159	-1309	+ 489	+ 951
67	3.94	.137	1.28	-2228	-1391	+ 530	+ 880
68	4.40	.137	1.04	-2353	-1486	+ 513	+ 914
Test Pile 3 (95 ft long)							
7	5.14	3.23		-2573	-1840	+1496	+ 526
8	5.12	2.98		-2559	-2086	+1510	+ 695
10	4.92	2.46		-2503	-2188	+1568	+ 685
12	4.74	1.56		-2462	-2220	+1464	+ 726
17	4.25	.531	1.34	-2310	-2030	+1141	+ 915
35	3.94	.344	4.99	-2200	-1932	+ 708	+ 920
40	3.48	.273	2.90	-2037	-1434	+ 488	+ 606
45	4.19	.266	2.81	-2283	-2147	+ 621	+ 869
50	3.78	.206	2.34	-2145	-1932	+ 470	+ 828
55	4.19	.180	1.91	-2283	-1973	+ 549	+ 807
60	4.09	.127	1.60	-2241	-2119	+ 477	+ 818
65	4.18	.145	1.61	-2283	-2137	+ 600	+ 850
67	4.02	.137	.890	-2228	-2065	+ 530	+ 808
68	4.42	.137	.460	-2353	-2326	+ 513	+ 552
69	4.36	.128	.233	-2340	-2149	+ 414	+ 532
70	4.48	.139	.135	-2262	-2260	+ 365	+ 348
74	4.48	.104	.055	-2367	-2168	+ 321	+ 296
Test Pile 4 (92 ft long)							
20	3.96	.757	.923	-2232	-1460	+1020	+ 526
23	3.73	.666	12.0	-2132	-1746	+ 893	+ 938

*Compressive Stresses were taken at head of pile. Tension Stresses were taken at mid-point of pile unless noted otherwise.

TABLE 4 (Continued)

Depth of Pile in Ground ft	Computed Hammer Drop ft	Average Penetration Per Blow in		Comparison of Computed Stresses With Average Measured Stresses			
		Comp.	Meas.	- Compression		+ Tension	
		Comp.	Meas.	Comp.	Meas.	Comp.	Meas.
46	4.14	.268	2.40	-2275	-1972	+ 524	+ 825
50	4.22	.246	.308	-2375	-1939	+ 588	+ 678
52	4.23	.220	.154	-2304	-1981	+ 528	+ 554
53	4.39	.220	.138	-2361	-1997	+ 562	+ 427
54	4.38	.207	.190	-2318	-1961	+ 528	+ 456
55	4.02	.198	.247	-2304	-1645	+ 515	+ 668
56	4.02	.183	.308	-2232	-1672	+ 455	+ 719
57	4.20	.180	.353	-2261	-1759	+ 472	+ 916
66	4.69	.144	.364	-2447	-1850	+ 313	+ 417
69	4.74	.127	.104	-2418	-1912	+ 242	+ 399

Test Pile 5 (92 ft. long)

5	3.88	3.13		-2203	-1565	+ 975	+ 734
10	3.74	1.88	1.00	-2132	-1578	+ 846	+ 762
15	3.70	1.18	3.00	-2118	-1557	+ 845	+ 795
20	3.90	.757	.705	-2232	-1638	+ 771	+ 726
25	3.90	.489	4.00	-2189	-1700	+ 615	+ 802
40	3.94	.318	2.00	-2203	-1632	+ 434	+ 632
50	4.43	.246	.364	-2375	-1809	+ 365	+ 543
55	4.90	.198	.292	-2304	-1741	+ 322	+ 368
57	4.10	.180	.480	-2261	-1695	+ 318	+ 532
58	4.10	.175	.667	-2261	-1720	+ 322	+ 645
65	4.13	.136	.750	-2275	-1547	+ 435	+ 495
67	4.66	.139	.400	-2447	-1910	+ 446	+ 530
68	4.69	.133	.150	-2432	-1925	+ 465	+ 426
69	4.60	.127	.074	-2418	-1829	+ 477	+ 279

Test Pile 6 (26 ft long)

2	3.73			-2248	-1404	+ 578	+ 293 (gage 4)
3	5.07			-2951	-2433	+1201	+ 433
12	4.54			-2760	-2104	+ 798	+ 342
15	5.22			-3004	-2512	+ 476	+ 358 (gage 4)
19	5.58			-3127	-2681	+ 496	+ 354 (gage 4)
20	5.57			-3125	-2761	+ 499	+ 346 (gage 4)
22.5	6.10	0.72	0.69	-3300	-3038	+1004	+ 402
24	5.91			-3250	-2894	+ 987	+ 407

Test Pile 7 (26 ft long)

2	3.28			-2251	-1394	+ 798	+ 452
11	4.74			-2835	-2050	+ 933	+ 361
15	5.23			-3004	-2333	+ 476	+ 441
18	5.48	0.85	0.66	-3105	-2470	+ 854	+ 415
19	5.27	0.74	0.53	-3022	-2486	+ 804	+ 442
20	5.50			-3101	-2592	+ 842	+ 428
25	5.50			-3124	-2680	+ 941	+ 449

pile length, soil resistance, and distribution of soil resistance on the driving stresses in a permanent set of concrete piling. Some 2106 problems were analyzed in this study and the results have been presented in the form of graphs in another publication.¹³

An example of these graphs is shown by Figures 21, 22, and 23. Figure 21 shows the effects of ram weight, ram energy output, and cushion stiffness on the driving stress in the given 65 ft long pile. It can be seen that for a given ram energy output a heavy ram produces lower tensile and compressive stresses than a light ram. A thick or soft cushion block is very effective in reducing both tensile and compressive stresses.

Figure 22 shows the effects of ram weight, ram energy output, and distribution of soil resistance on the driving stresses in the given 65 ft long pile. The tensile stresses produced in the friction piles are higher than those in the point bearing pile. This is what would be expected, since a large percentage of the initial compressive wave is reflected from the pile point as tension when little or no point resistance is encountered. No consistent change can be noted in the compressive stresses.

Figure 23 shows the effect of ram weight and ram energy output on the permanent set of the given 65 ft long pile. For a given ram energy output a heavy ram produces considerably more permanent set than a light ram. This observation shows one reason why existing simplified pile formulas cannot reliably predict soil resistance from a given penetration.

CONCLUSIONS

As a result of the field tests of dynamic stresses in and displacements of prestressed concrete piles during driving, the following conclusions are drawn:

1. Maximum compressive stresses occurred at the head of the piles tested when firm resistance to penetration was encountered. Typical measured values ranged from 2,000 to 3,350 psi.
2. Maximum tensile stresses were found to occur at the mid-point and lower half of the piles. For the 95 ft and 92 ft piles tested, measured values ranged from 900 to 1,350 psi. For the 26 ft long piles, measured values ranged from 300 to 696 psi. The actual net tensile stress in the concrete is obtained by subtracting the prestress from the measured values.

¹³Hirsch, T.J., "Computer Study of Variables Which Affect the Behavior of Concrete Piles During Driving," Report of the Texas Transportation Institute, Texas A&M University, August, 1963.

3. Bending stresses may occur in long piles because the hammer is not centered on top of the pile, the pile is crooked, the pile is not vertical, and the top of the pile is out of square. Bending stresses associated with the compressive wave were measured at about ± 350 psi and those associated with the tensile wave were measured at about ± 150 psi.

4. The stresses and displacements computed by use of wave theory agreed fairly well with the measured data. It was indicated, however, that more research needs to be directed toward determining the dynamic properties of the wood, concrete, and soils involved.

As a result of the theoretical studies of dynamic stresses and displacements in prestressed concrete piles, the following additional conclusions are presented concerning driving conditions which are likely to produce very large stresses:

5. For a given ram energy output, a heavy ram produces lower tensile and compressive stresses than a light ram.

6. For a given ram energy output, a heavy ram produces more permanent set than a light ram.

7. A soft cushion is very effective in reducing both tensile and compressive stresses in a pile.

8. A light or weak soil resistance produces larger tensile stresses in a pile than a hard or strong soil resistance.

9. In general, the tensile stresses produced in friction piles are higher than those in point-bearing piles. No consistent change can be noted in the compressive stresses.

10. In general, long piles have higher tensile stresses than short piles. The length of the pile has no significant effect on the compressive stresses.

11. Increasing the cross-sectional area of a pile produces a slight decrease in the axial compressive stress, but no consistent change is noted in the axial tensile stress. Because of the higher slenderness ratio, the bending stresses due to imperfect driving conditions may be increased, however.

Any variables not mentioned in the specific conclusion above are assumed to be constant.

ACKNOWLEDGMENTS

The field tests described in this paper were conducted as a part of Research Projects RP-27 and HPS 1(27)L. The first project was sponsored by the Bridge Division of the Texas Highway Department and the latter was sponsored jointly by the Bridge Division of the Texas Highway Department and the Bureau of Public Roads. The wave-theory computer program was obtained as a part of Research Project RP-25 sponsored by the Bridge Division of the Texas Highway Department. All three projects were conducted by the Texas Transportation Institute, Texas A&M University. The authors gratefully acknowledge the assistance of Farland C. Bundy, Supervising Design Engineer, Bridge Division of the Texas Highway Department, who worked closely with the authors in accomplishing the projects.

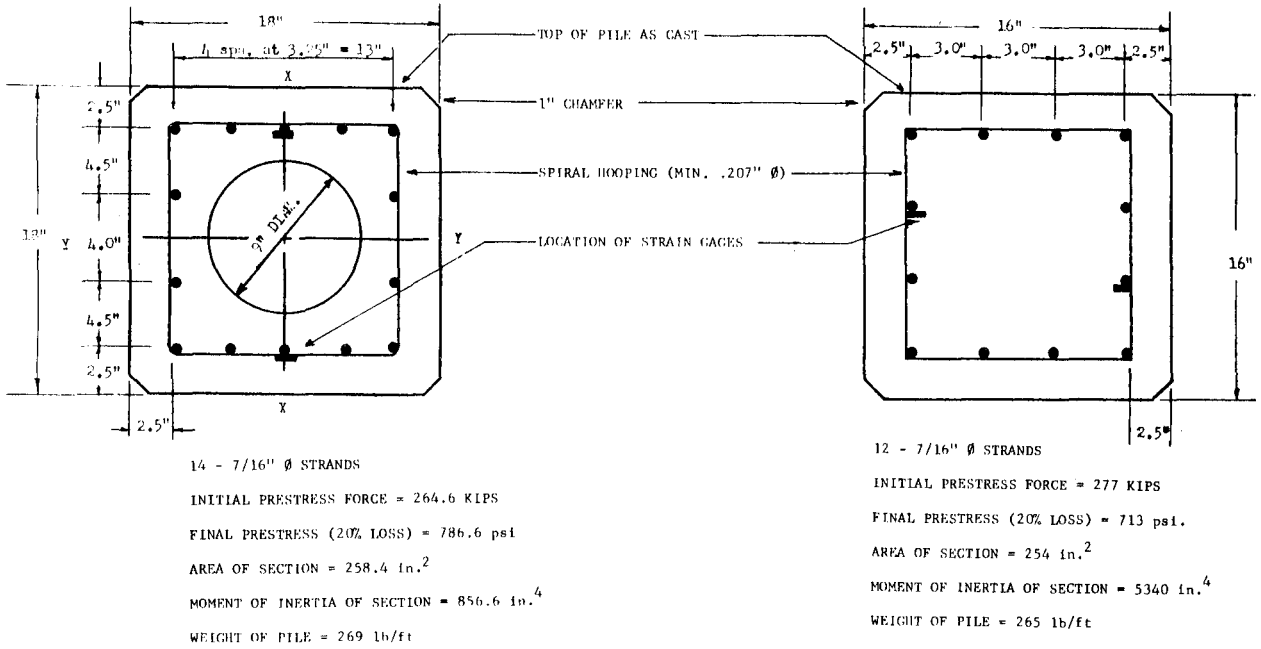
Appreciation is also extended to E.A.L. Smith who maintained a continuing interest and contributed much effort throughout this work.

Acknowledgement is also due Ross Anglin and Son (General Contractors), Brown and Root Company, and Baass Brothers Concrete Company, all of Texas, for their cooperation in the field tests. Thanks are also due the California Company of New Orleans, La., for use of their recording oscillograph and amplifiers.

REFERENCES

1. Samson, Charles H., Jr., "Pile-Driving Analysis by the Wave Equation (Computer Procedure)," Report of the Texas Transportation Institute, Texas A&M University, May, 1962.
2. Samson, C. H., Hirsch, T. J., and Lowery, L. L., "Computer Study of Dynamic Behavior of Piling," a paper presented to Third Conference on Electronic Computation, ASCE, Boulder, Colorado, June, 1963.
3. Hirsch, T. J., "Stresses in Long Prestressed Concrete Piles During Driving," Report of the Texas Transportation Institute, Texas A&M University, September, 1962.
4. Glanville, W. H., Grime, G., Fox, E. N., and Davies, W. W., "An Investigation of the Stresses in Reinforced Concrete Piles During Driving," British Building Research Board Technical Paper No. 20, Dept. of Scientific and Industrial Research, His Majesty's Stationery Office, London, 1938.

5. "Steel and Timber Pile Tests-West Atachafalaya Floodway- New Orleans, Texas and Mexico Railway," American Railway Engineering Association, Bulletin 489, September-October, 1950.
6. "Delmag Diesel Pile Hammers-Technical Data," Goddard Machinery Company, Inc., Houston, Texas.
7. Rands, Morgens, "Test Performed with the Delmag Diesel Hammer, Type D-12," Dept. of Mechanical Engineering, University of Toronto, December, 1955.
8. Smith, E. A. L., "Pile-Driving Analysis by the Wave Equation," Journal of the Soil Mechanics and Foundations Division, Proceedings of the American Society of Civil Engineers, Volume 86, Number SM 4, pp. 35-61, August, 1960.
9. Hirsch, T. J., "Computer Study of Variables Which Affect the Behavior of Concrete Piles During Driving," Report of the Texas Transportation Institute, Texas A&M University, August, 1963.
10. Hirsch, T. J., "Field Tests of Prestressed Concrete Piles During Driving," Report of the Texas Transportation Institute, Texas A&M University, August, 1963.
11. Rand, Morgens, "How the Diesel Pile Hammer Works," Roads and Streets, May, 1961.



TEST PILES 1,2,3,4 & 5

TEST PILES 6 & 7

FIGURE 1 CROSS - SECTION OF TEST PILES

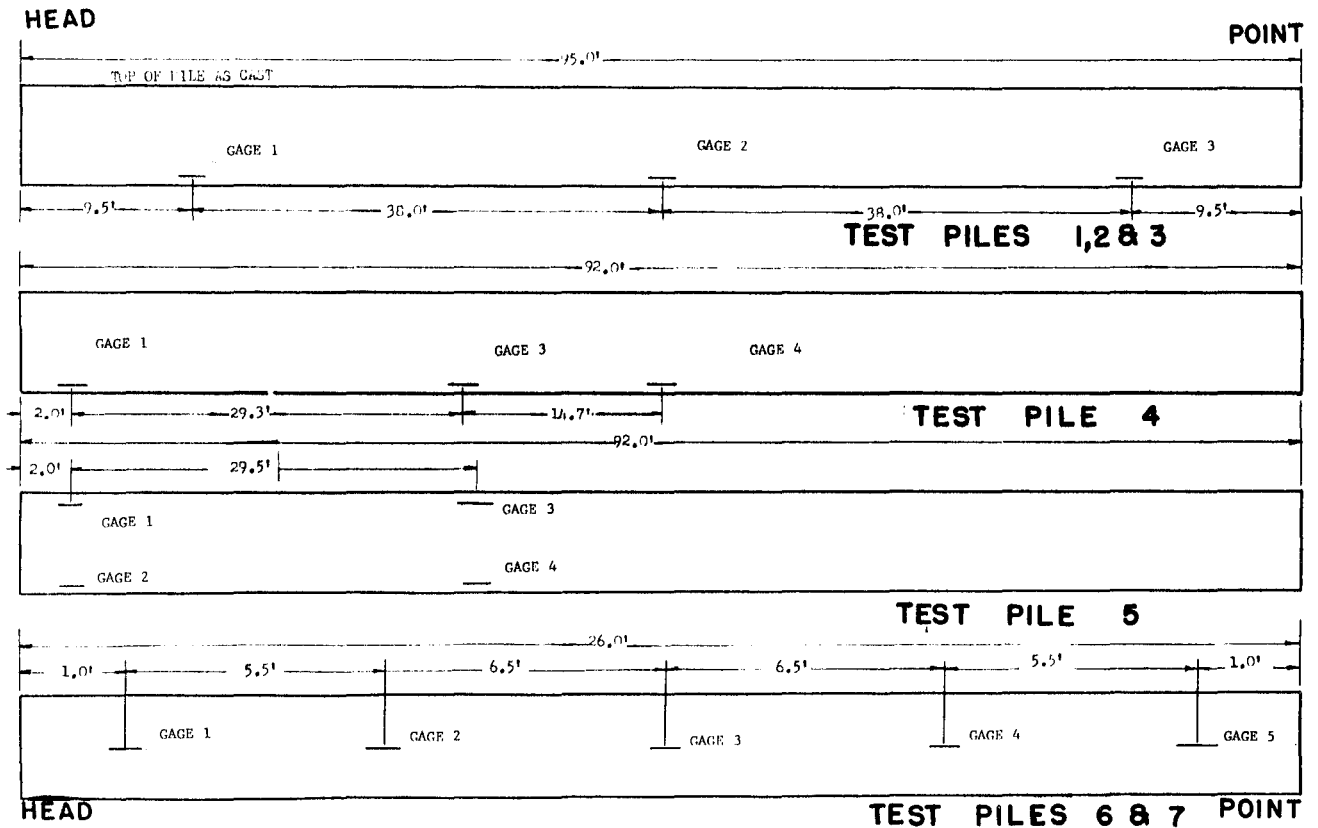


FIGURE 2 SIDE VIEW OF TEST PILES

ULTIMATE SHEAR STRENGTH OF SOIL IN KIPS PER LINEAR FOOT OF PILE

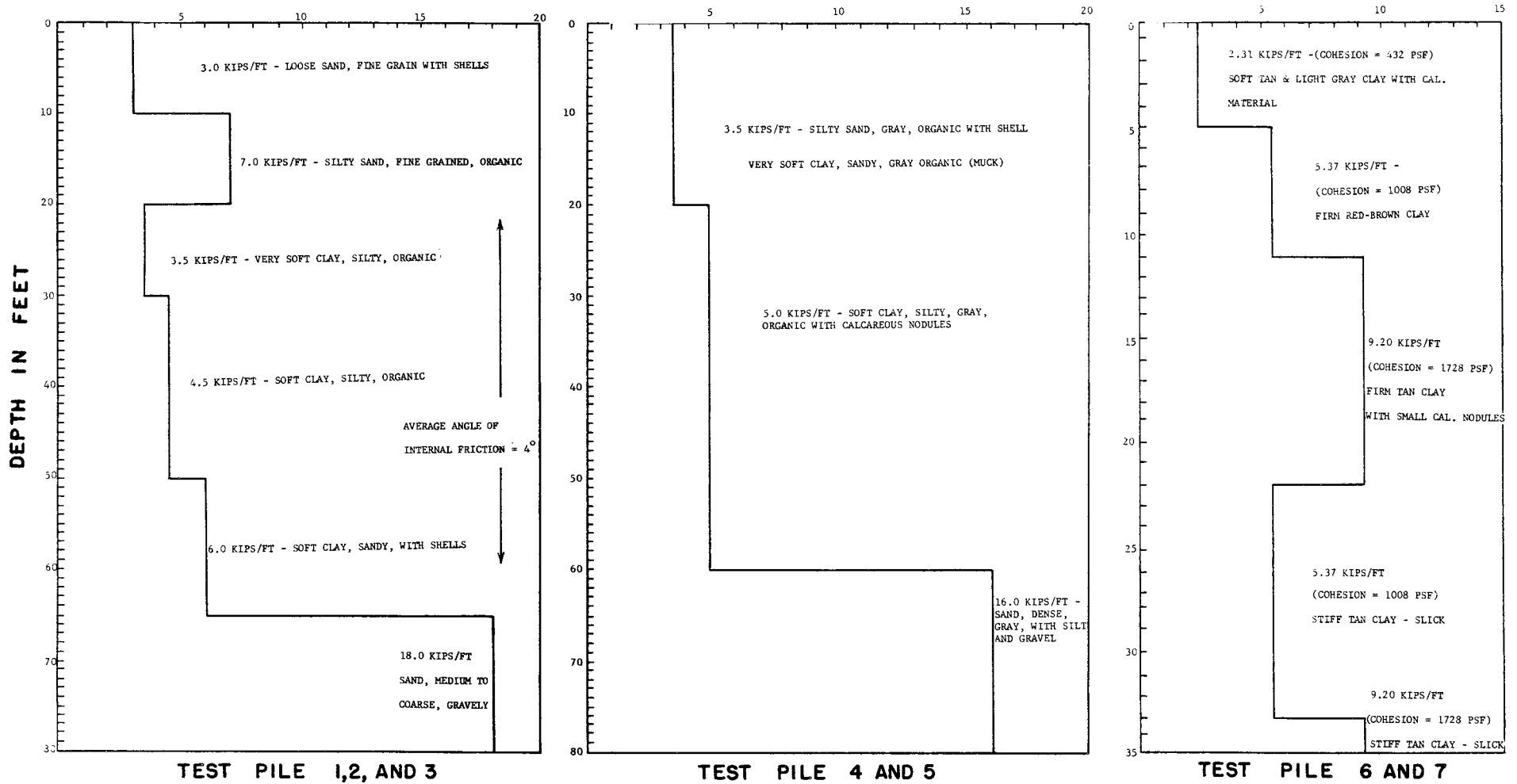
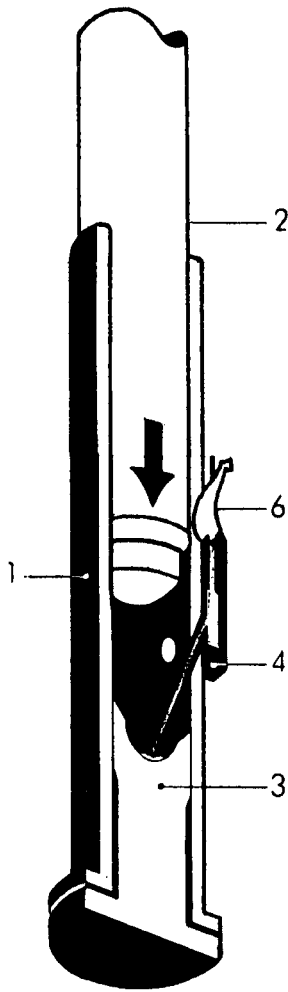


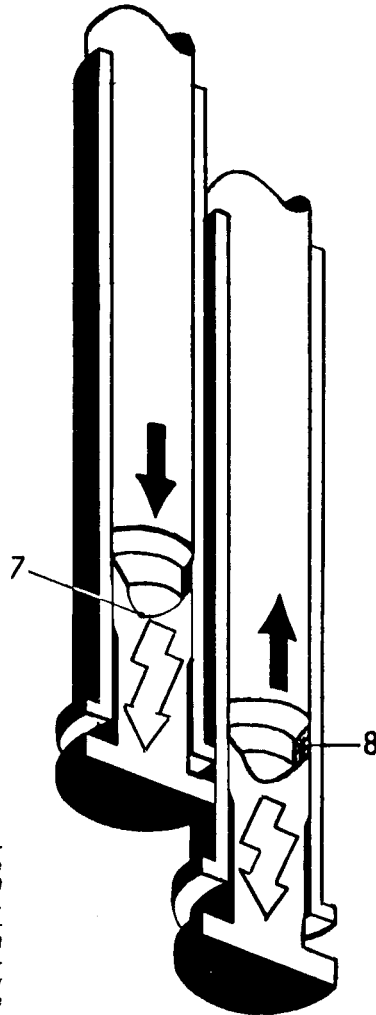
FIGURE 3. ULTIMATE SHEAR STRENGTH OF SOIL AT VARIOUS DEPTHS IN GROUND

Free fall



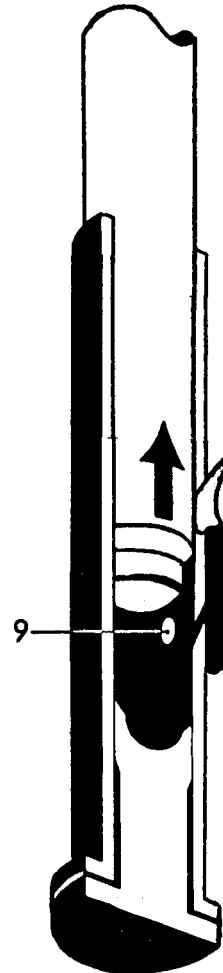
1. The long cylinder (1) accommodates in its upper half the piston (2) and the impact block (3) in its lower part. The piston is the actual working part, whereas the impact block rests on the pile to impart the energy, produced by the falling piston and the explosion, to the pile. The impact block also serves to seal off the combustion chamber at the lower end. To start the hammer the piston (2) is lifted and, when reaching a certain height, is automatically released. During the downward fall of the piston (2) a pump lever (6) on the fuel pump (4) is activated injecting a fixed amount of Diesel fuel into the combustion chamber.

Blow plus Explosion



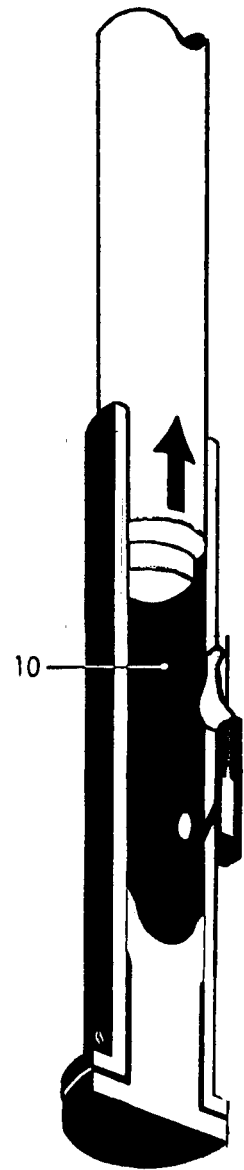
2. As the piston (2) continues to fall it closes the exhaust ports, compresses the remaining air in the cylinder and hits the concave ball pan of the impact block. The impact of the falling piston (2) atomizes the Diesel fuel lying in the ball pan, and the highly compressed air causes these atomized fuel particles to ignite. The combustion pressure thus created exerts an additional force onto the pile, which is already travelling downward under the compression force developed by the falling piston, and the blow from the piston further serves to throw the piston (2) up for the next working cycle.

Exhaust



3. As the piston clears the exhaust ports (9) in its upward motion the internal and external pressures are equalized.

Scavenging



4. As the piston continues its upward motion fresh air is drawn into the cylinder (10), which is thus being scavenged.

Figure 4. Working Principle of Delmag Diesel Pile Hammers

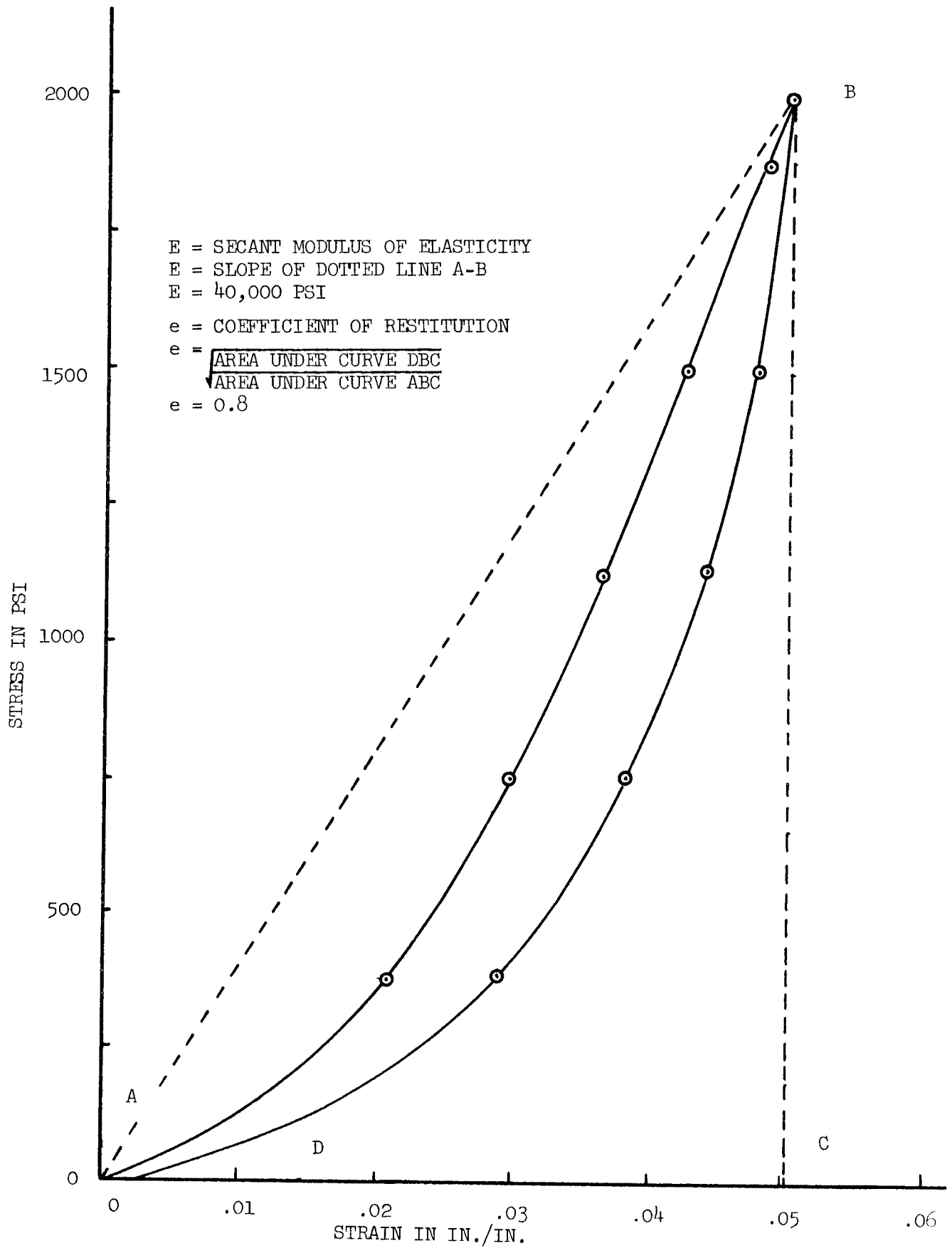


FIGURE 5. Typical static stress - strain curve for compressed green oak loaded perpendicular to its grain.



Figure 6. Delmag D-22 diesel hammer driving prestressed concrete pile.

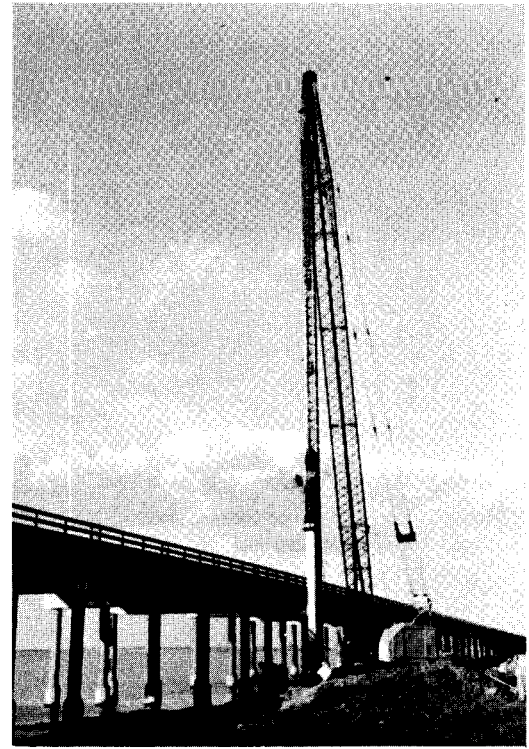


Figure 7. View of 95' pile leads used to drive piles up to 115' in length.

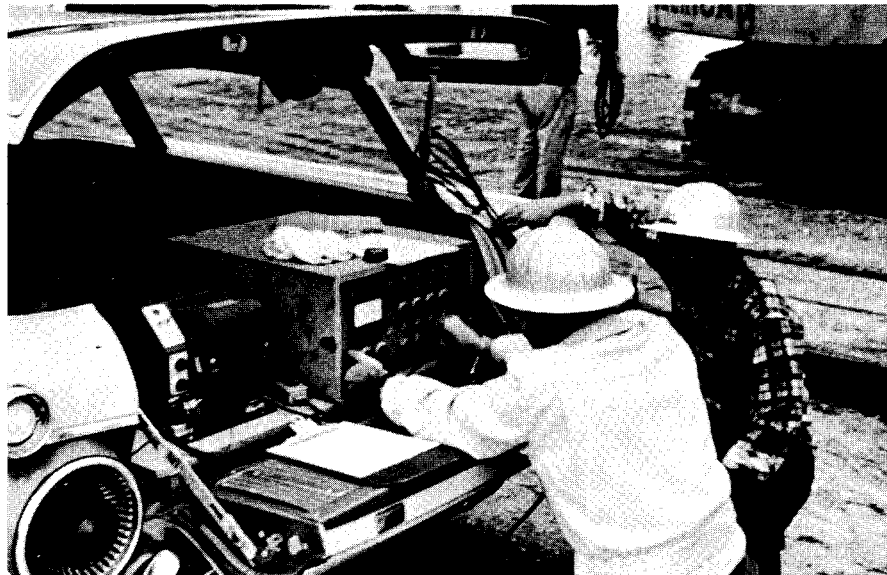


Figure 8. Recording oscillograph and strain gage amplifier unit recording strains from gages embedded in concrete piles during driving on Nueces Bay Causeway, near Corpus Christi, Texas.

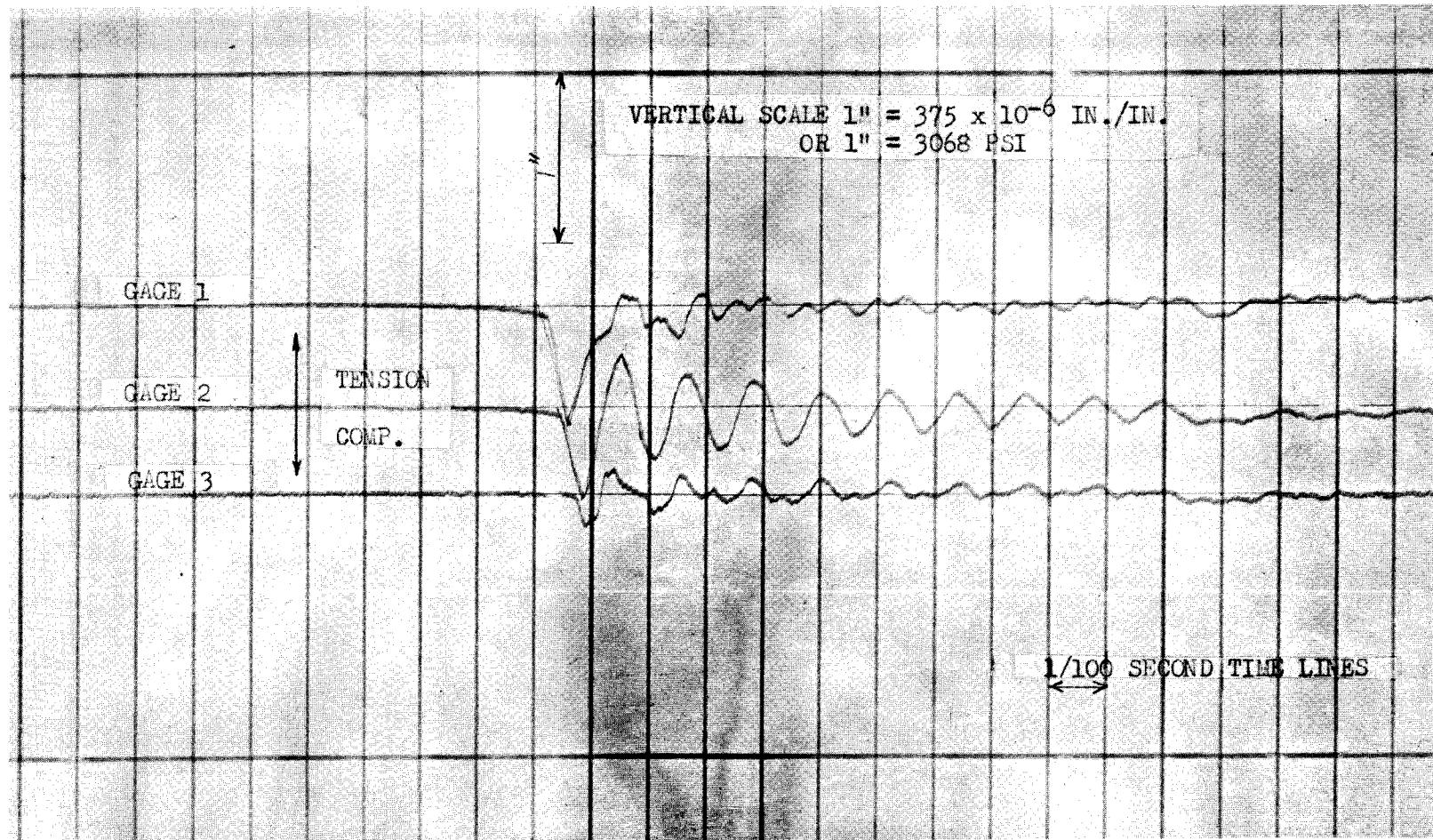


Figure 9. Oscillograph strain record from Test Pile 3. 18 in. square prestressed concrete pile 95 ft. long, pile penetration 45 ft. in ground.

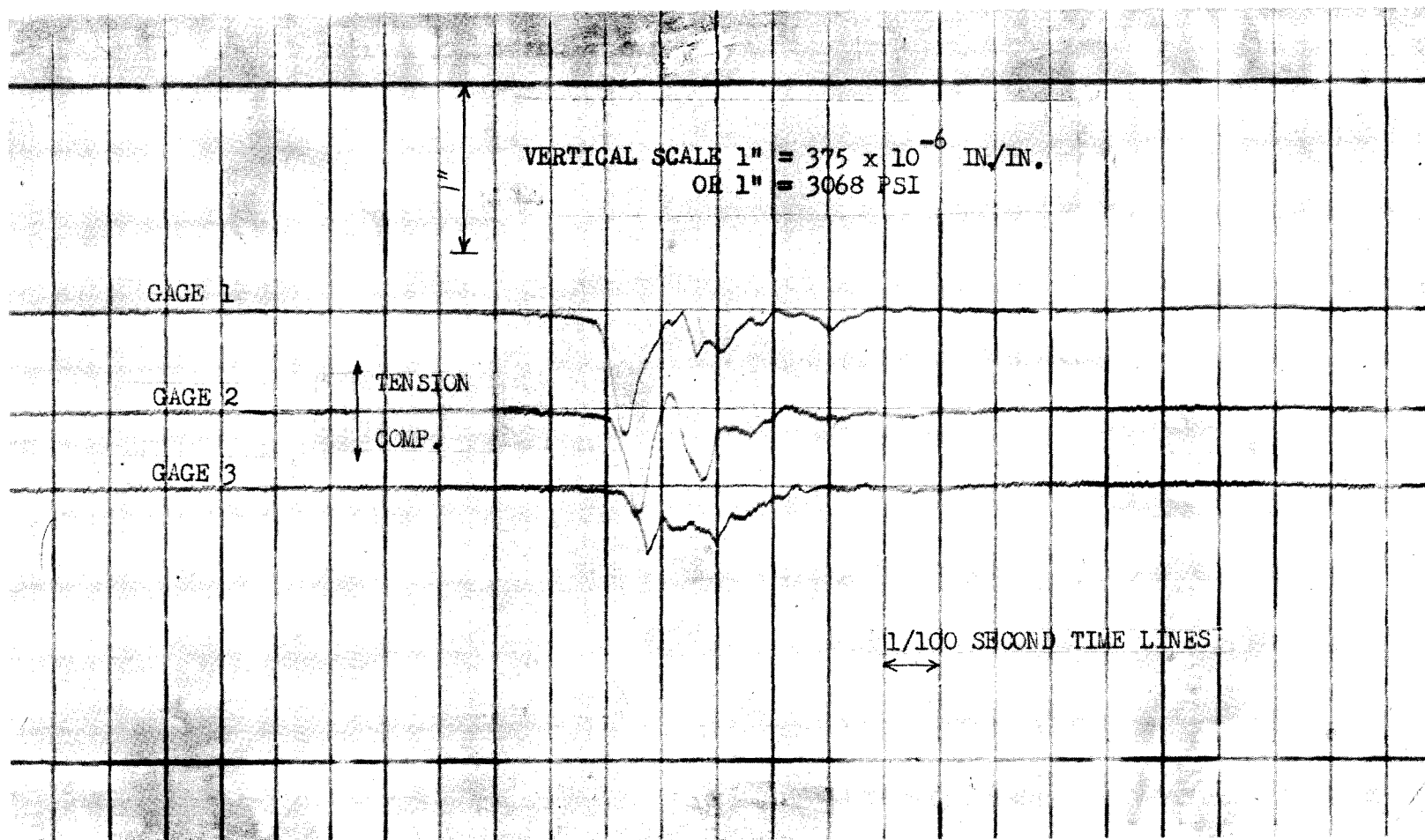


Figure 10. Oscillograph strain record from Test Pile. 18 in. square prestressed concrete pile 95 ft. long, pile penetration 74 ft. in ground.

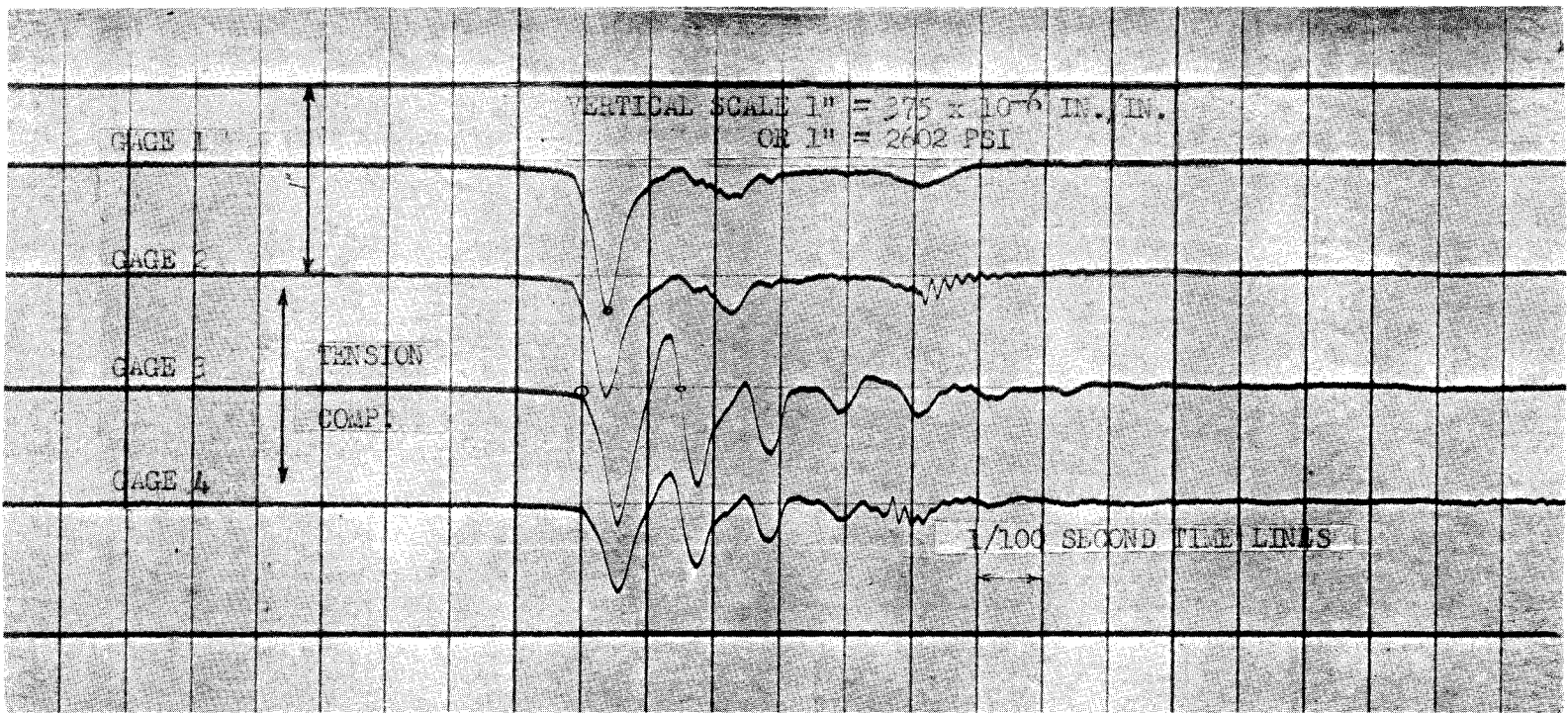


Figure 11. Oscillograph strain record from Test Pile 5. 13 in. square prestressed concrete pile 92 ft. long, pile penetration 50 ft. in ground.

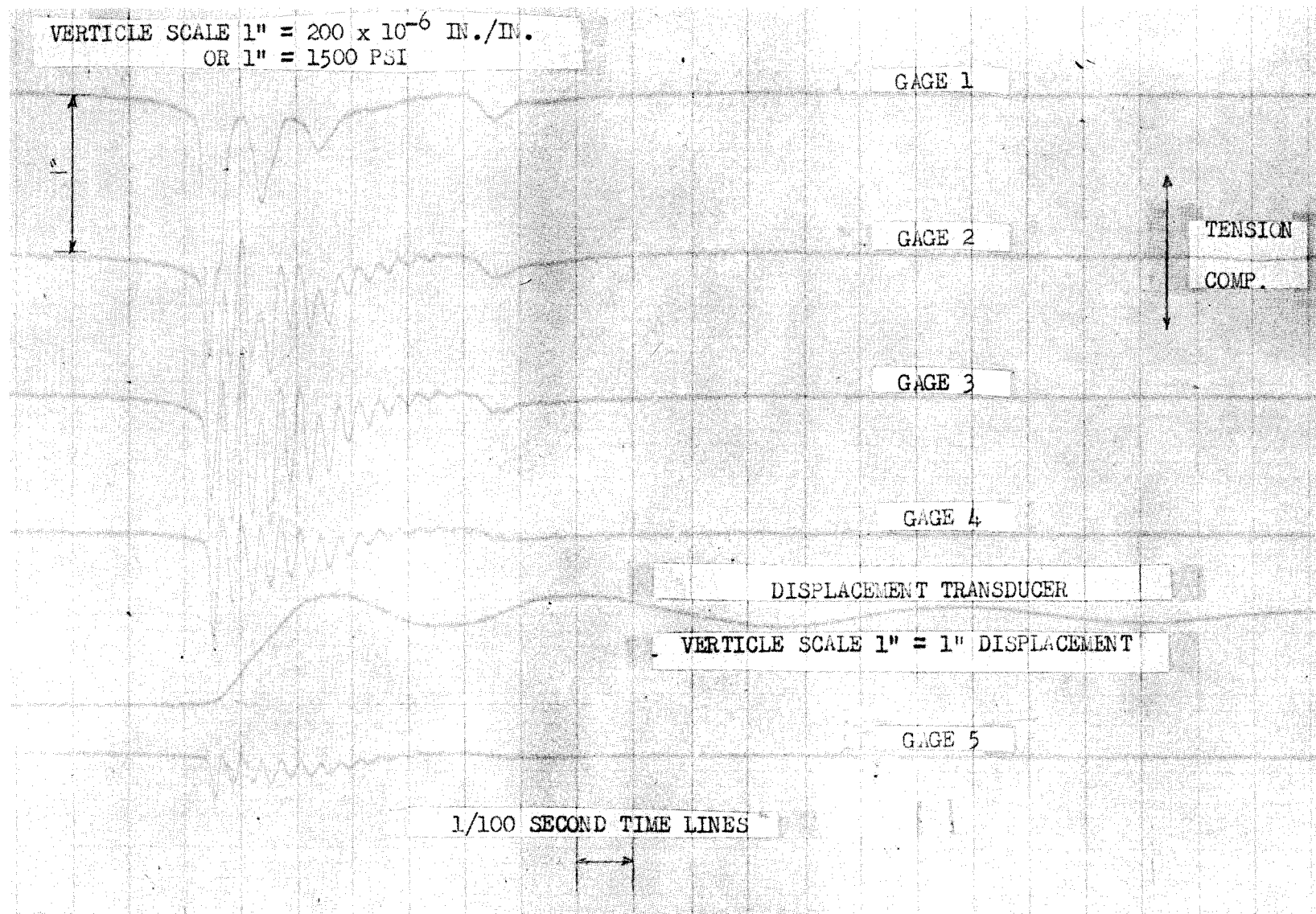


Figure 12. Oscillograph strain record from Test Pile 7. 16 in. square prestressed concrete pile 26 ft. long, pile penetration 19 ft. in ground.

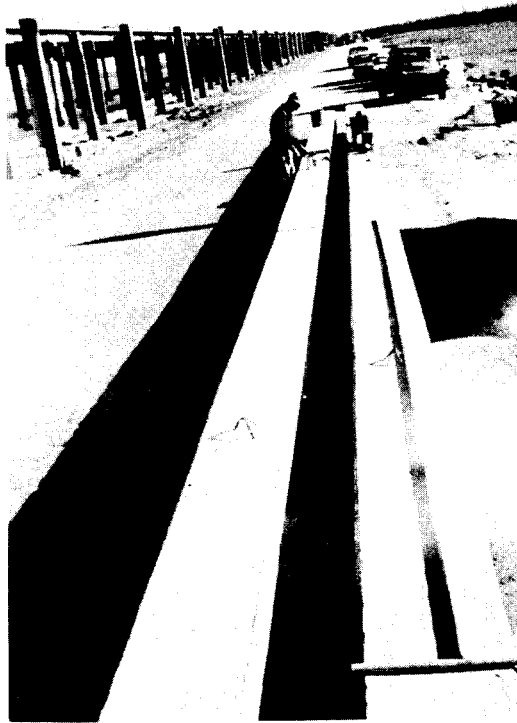


Figure 13. Two 95' prestressed concrete piles which broke in tension while being driven. Workman is applying epoxy to cracks which were perpendicular to longitudinal axis of pile. All cracks occurred in lower half of piles.

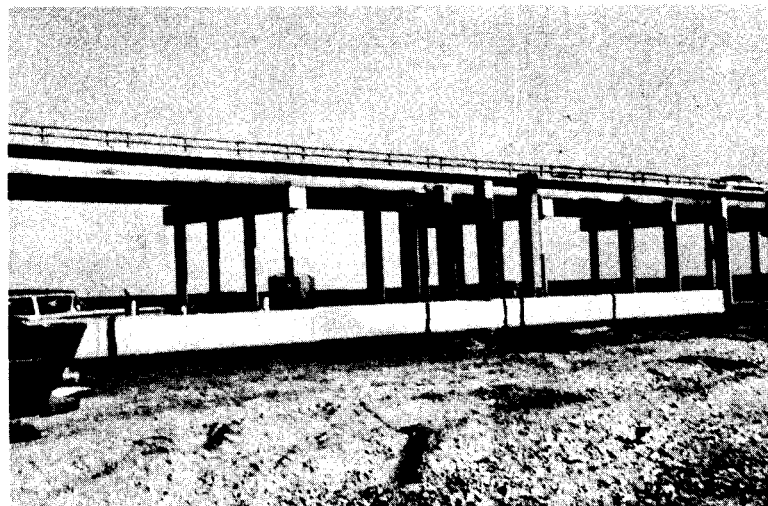


Figure 14. View of lower half of broken pile.

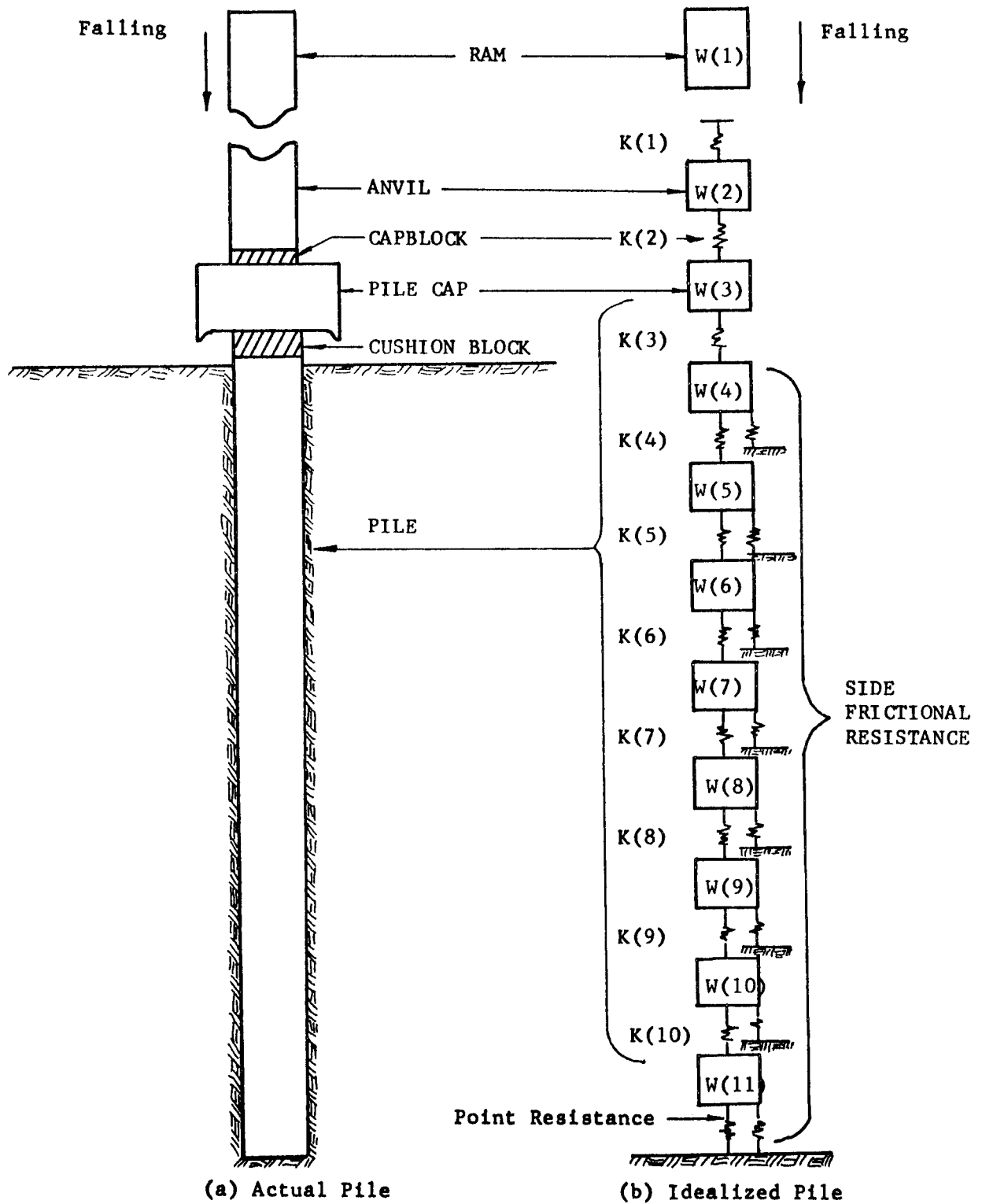


Figure 15. Method of idealizing a pile for purpose of analysis. This pile was divided into eight segments of equal lengths. Segment 1 is the ram, 2 is the anvil, 3 is the helmet, and 4 is the first segment of the pile.

S
T
R
E
S
S

I
N

P
S
I

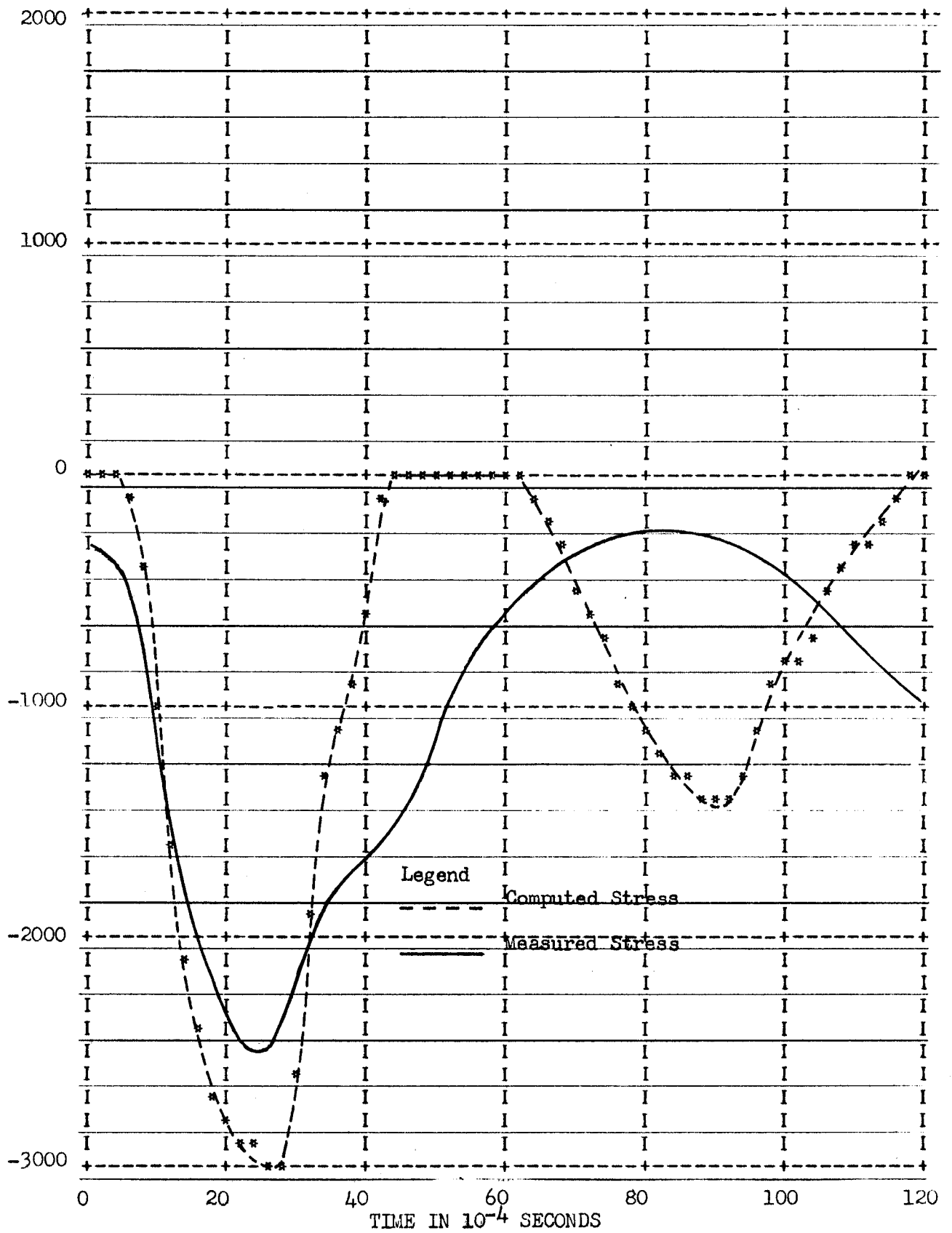


FIGURE 16. Stress at Pile Head vs Time
Test Pile 7, 19 ft. Penetration in ground.

S
T
R
E
S
S

I
N
P
I
L
E

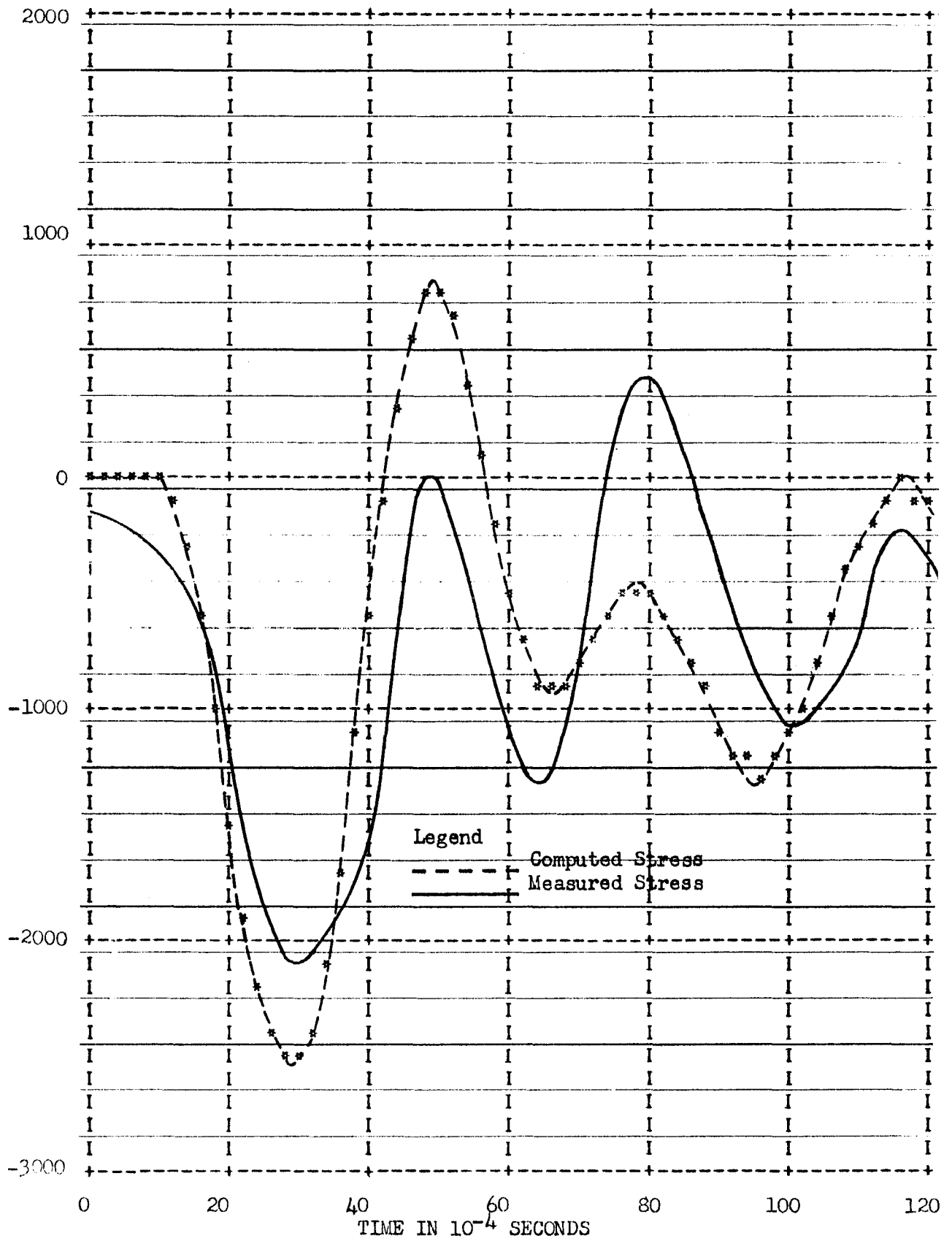


FIGURE 17. Stress at Mid-Length of Pile vs Time
Test Pile 7, 19 ft. Penetration in Ground

S
T
R
E
S
S

I
N

P
S
I

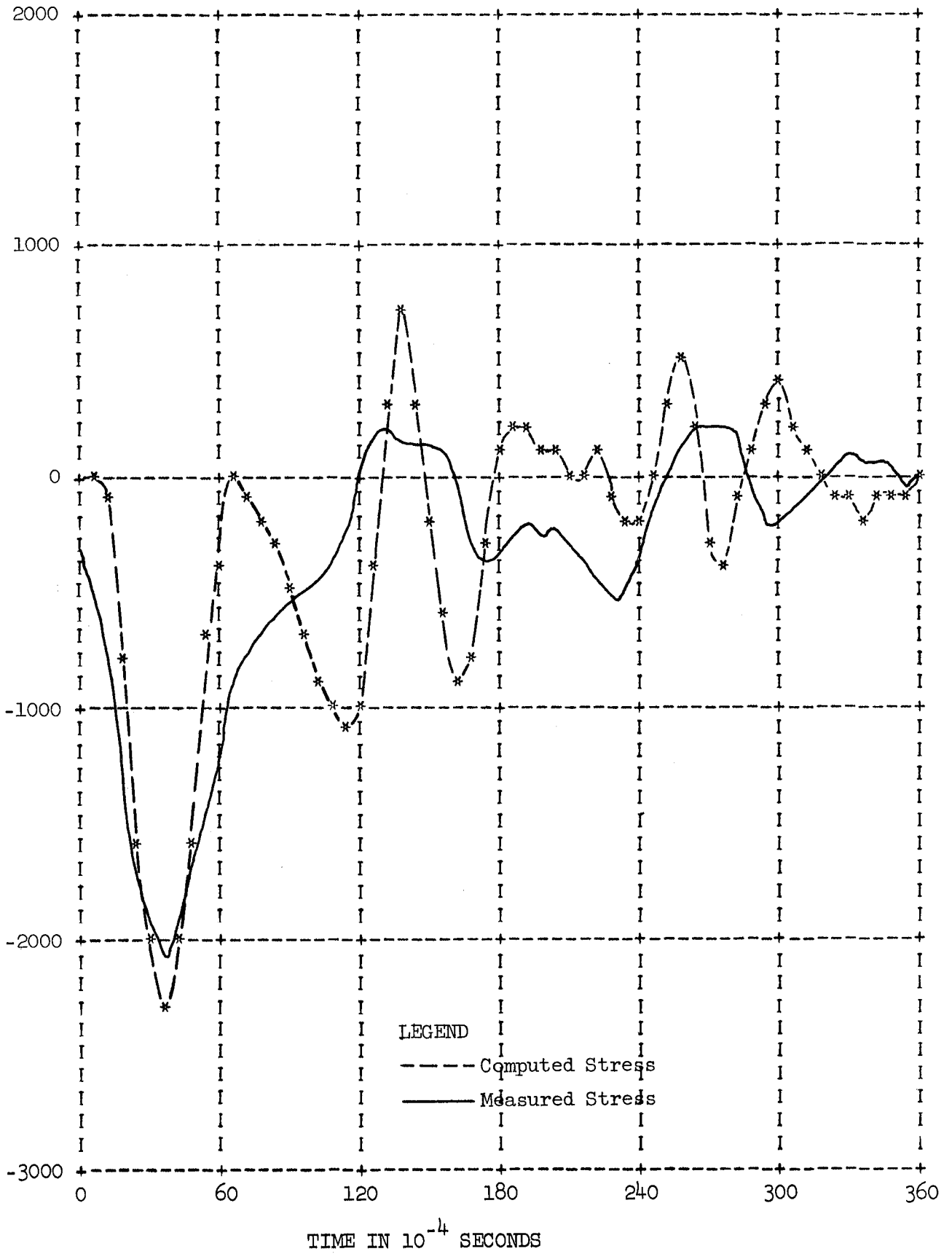


FIGURE 18. Stress in Pile Head $\frac{VS}{Time}$
Test Pile 3, 45' Penetration in Ground

S
T
R
E
S
S

I
N

P
S
I

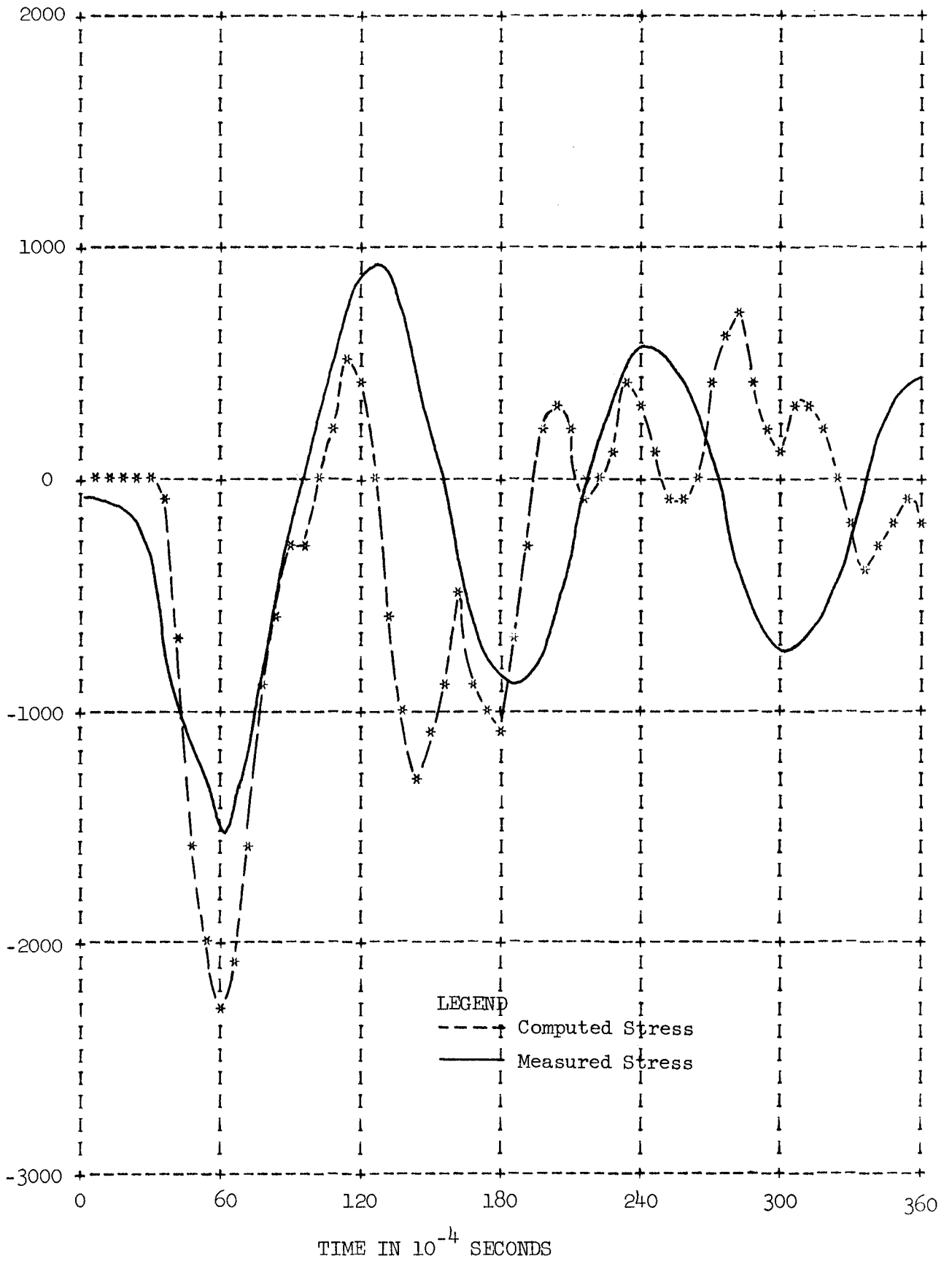


FIGURE 19. Stress at Mid-Length of Pile $\frac{vs}{Time}$
Test Pile 3, 45' Penetration in Ground

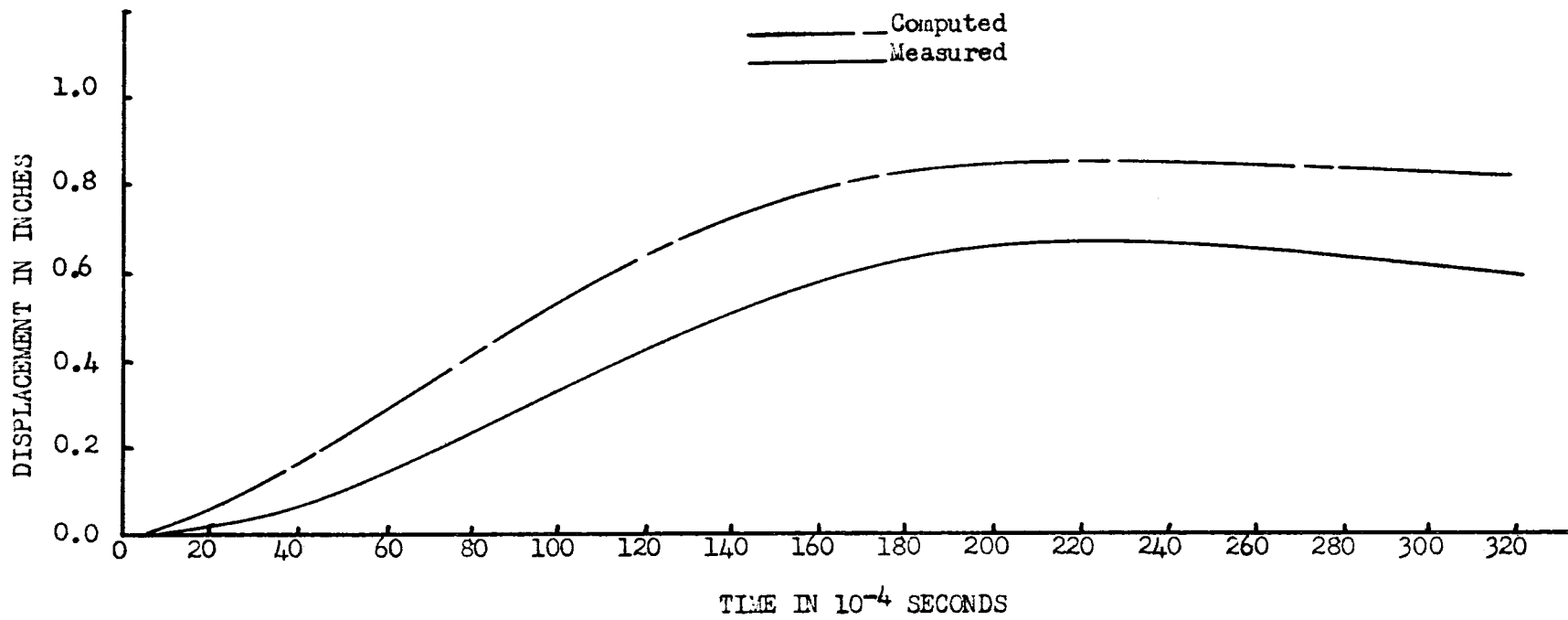


Figure 20. Displacement of pile head vs time
Test Pile 7, 19 ft. penetration in the ground.

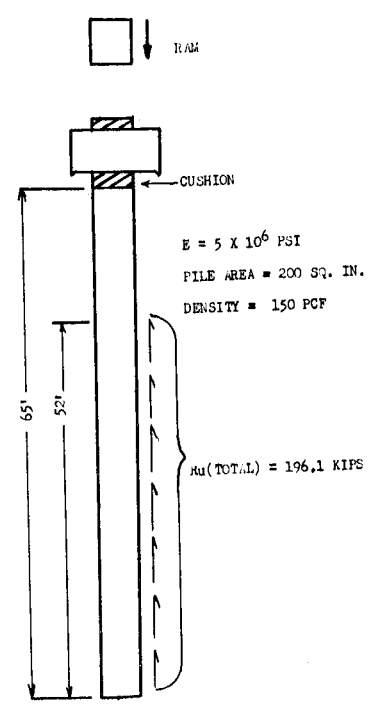
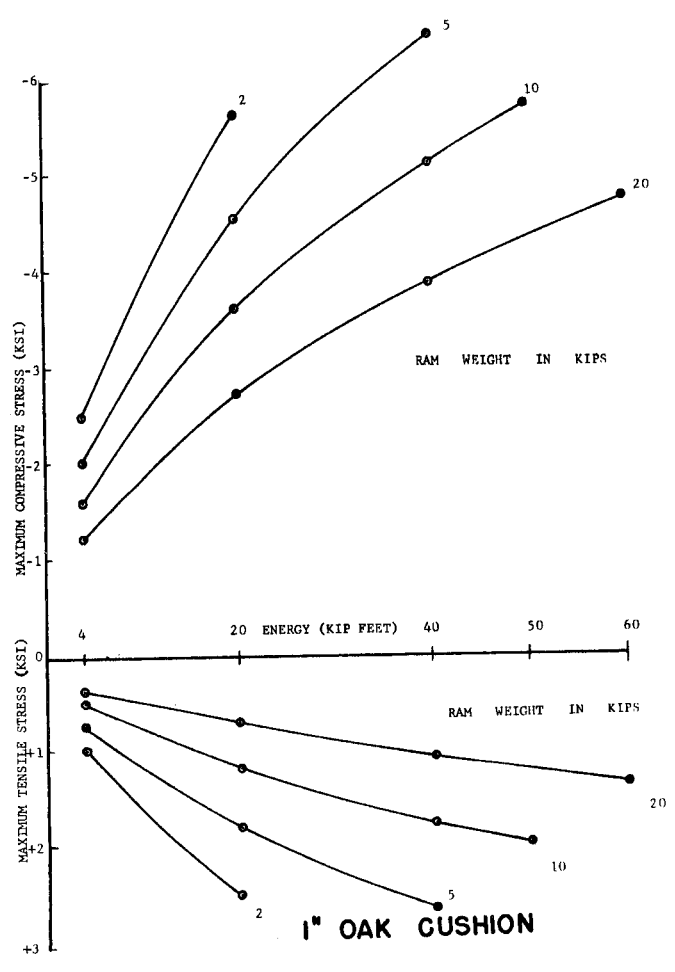
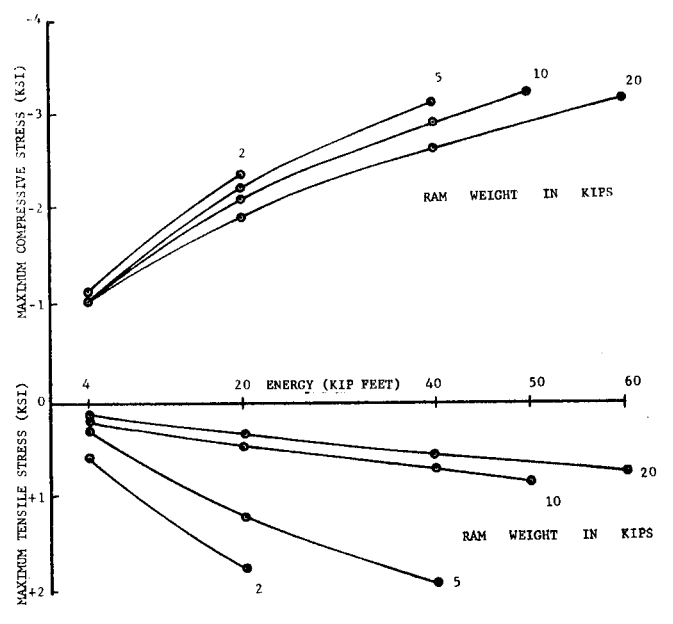
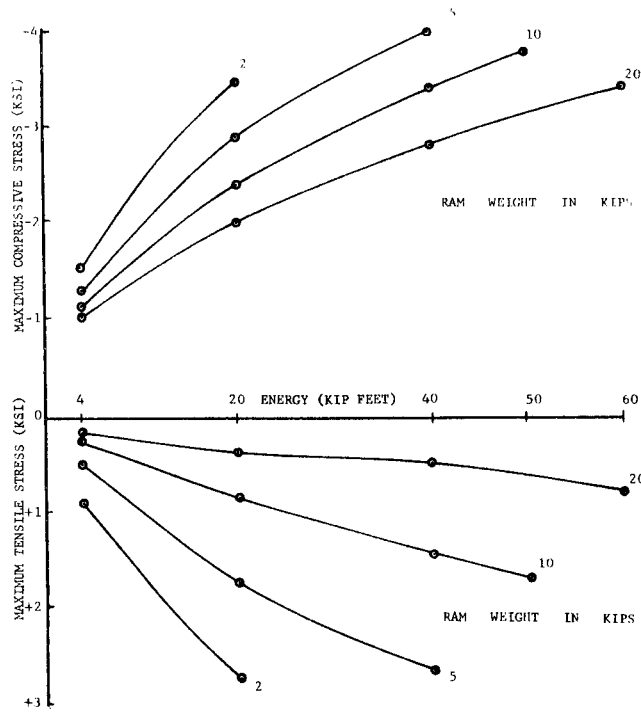
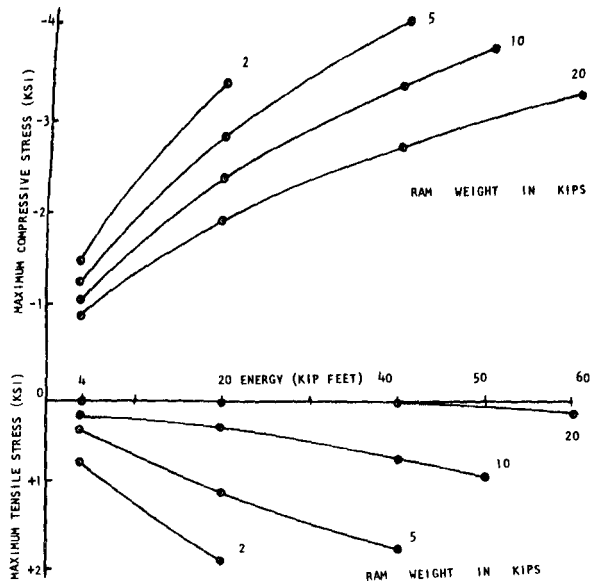
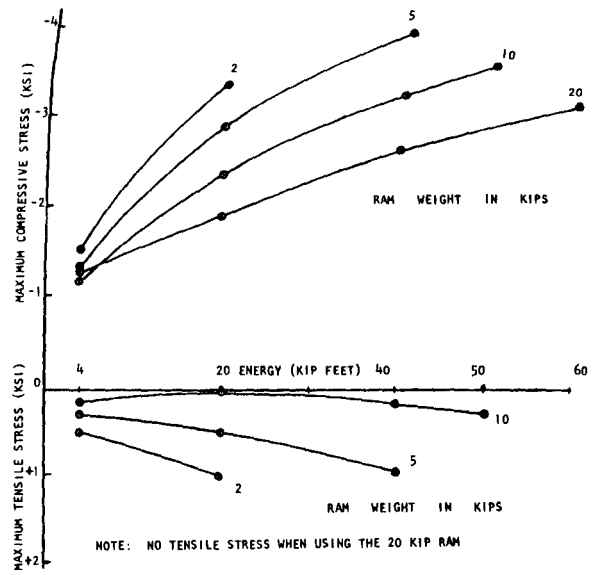


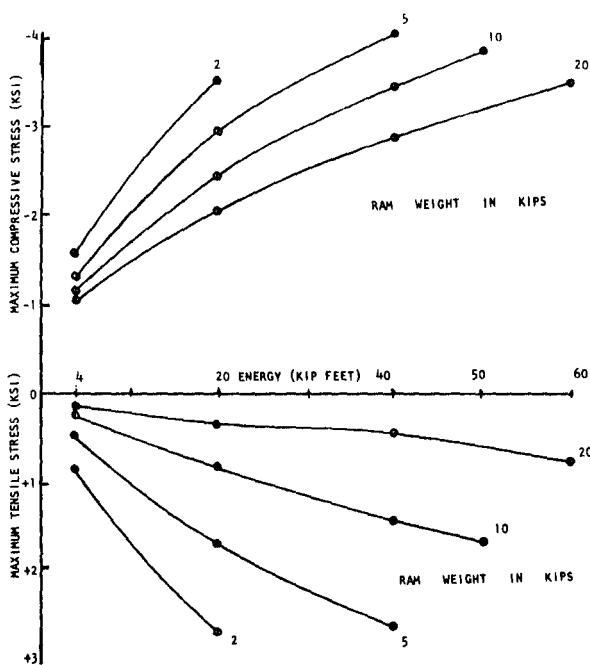
FIGURE 21. EFFECT OF CUSHION STIFFNESS ON PILE STRESSES



1/2 POINT & 1/2 FRICTION



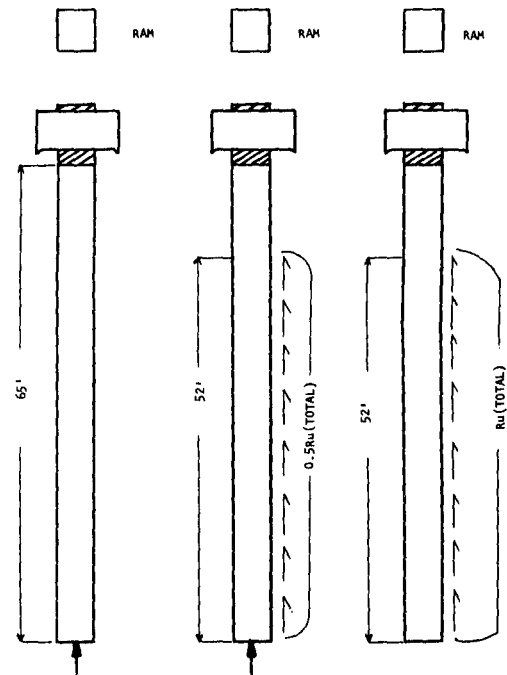
POINT



FRICTION

AREA = 200 SQ. IN.
DENSITY = 150 PCF.

$E = 5 \times 10^6$ PSI
CUSHION = 3" OAK



$R_u(TOTAL) = 196.1$ KIPS

POINT 0.5 POINT & 0.5 FRICTION FRICTION

FIGURE 22. EFFECT OF DISTRIBUTION OF SOILS RESISTANCE ON PILE STRESSE